

# Paradigm shift in diffusion-mediated surface phenomena

Denis S. Grebenkov<sup>1,\*</sup>

<sup>1</sup> *Laboratoire de Physique de la Matière Condensée (UMR 7643),  
CNRS – Ecole Polytechnique, IP Paris, 91128 Palaiseau, France*

(Dated: July 23, 2020)

Diffusion-mediated surface phenomena are crucial for human life and industry, with examples ranging from oxygen capture by lung alveolar surface to heterogeneous catalysis, gene regulation, membrane permeation and filtration processes. Their current description via diffusion equations with mixed boundary conditions is limited to simple surface reactions with infinite or constant reactivity. In this letter, we propose a probabilistic approach based on the concept of boundary local time to investigate the intricate dynamics of diffusing particles near a reactive surface. Reformulating surface-particle interactions in terms of stopping conditions, we obtain in a unified way major diffusion-reaction characteristics such as the propagator, the survival probability, the first-passage time distribution, and the reaction rate. This general formalism allows us to describe new surface reaction mechanisms such as for instance surface reactivity depending on the number of encounters with the diffusing particle that can model the effects of catalyst fooling or membrane degradation. The disentanglement of the geometric structure of the medium from surface reactivity opens far-reaching perspectives for modeling, optimization and control of diffusion-mediated surface phenomena.

Keywords: Diffusion-influenced reactions, Surface reaction mechanisms, Catalyst fooling, Dirichlet-to-Neumann operator, Boundary local time

The dynamics of particles near a reactive surface is critically important for many natural phenomena and industrial processes such as diffusion-mediated heterogeneous catalysis, biochemical reactions on DNA strands, proteins and cell membranes, filtration through porous media, permeation across membranes, surface relaxation in nuclear magnetic resonance, target searching and animal foraging, to name but a few [1–8]. In a typical setting, a particle (e.g., a molecule, an ion, a protein, a bacterium, an animal) moves inside a confining medium; when the particle comes close to the boundary of the medium, an appropriate surface mechanism can be initiated, e.g., the particle can bind to the boundary, relax its fluorescence, magnetization or another form of excitation, be chemically transformed into another molecule, be transported through a membrane pore, or be killed or destroyed (all these distinct mechanisms will be generically called “surface reaction” in the following). Whatever the surface mechanism is, its successful realization is not granted and depends on the state of the local environment near the particle. For instance, the boundary can be locally inert for binding, possess no catalytic germ or impurity for chemical transformation or relaxation; the closest membrane pore, channel or gate can be temporarily inactive or already occupied, while a predator can be asleep or not hungry; even if the target molecule or the escape hole is found, the particle may not overcome an energy activation or entropic barrier. In any of such unfavorable circumstances, the particle resumes its bulk motion until the next arrival to the boundary, and so on [9, 10]. As a consequence, the successful re-

alization of the surface reaction is typically preceded by a long sequence of successive bulk explorations, started and terminated on the surface (Fig. 1(a)). Even for ordinary bulk diffusion, partial surface reactivity results in very intricate and still poorly understood dynamics that affects the functioning of chemical reactors, living cells, exchange devices and organs such as lungs and placenta [1–13]. This dynamics becomes even more sophisticated for mortal walkers [14–16] that have a finite random lifetime due to, for instance, bulk relaxation, photobleaching, radioactive decay, bulk reaction, or starving.

The conventional description of these phenomena relies on macroscopic concentrations or, more fundamentally, on a propagator (also known as heat kernel or Green’s function),  $G_q(\mathbf{x}, t|\mathbf{x}_0)$ , that characterizes the likelihood of finding a particle that started from a point  $\mathbf{x}_0$  at time 0 and *survived* (not reacted) up to time  $t$ , in a bulk point  $\mathbf{x}$  at time  $t$ . The propagator obeys the Fokker-Planck equation, in which the bulk dynamics dictates the form of the Fokker-Planck operator, whereas the shape and the reactivity of the surface set boundary conditions [17]. For ordinary bulk diffusion, Collins and Kimball [18] put forward the Robin (also known as Fourier, radiation, or third) boundary condition

$$-D \partial_n G_q(\mathbf{x}, t|\mathbf{x}_0) = \kappa G_q(\mathbf{x}, t|\mathbf{x}_0), \quad (1)$$

where  $D$  is the diffusion coefficient and  $\partial_n$  is the normal derivative. At each boundary point, the net diffusive flux density from the bulk (the left-hand side) is equated to the reaction flux density, which is *postulated* to be proportional to  $G_q(\mathbf{x}, t|\mathbf{x}_0)$  on the boundary. The proportionality coefficient  $\kappa$  (in units of speed, m/s) bears the names of reactivity, permeability, relaxivity, or inverse surface resistance [19, 20], and can be related to the on-rate constant  $k_{\text{on}}$  of chemical reactions [21–23], to the microscopic

---

\*Electronic address: [denis.grebenkov@polytechnique.edu](mailto:denis.grebenkov@polytechnique.edu)

heterogeneity of catalytic germs [24–27], to the opening dynamics of gates, channels or pores [28, 29], to the energy activation or entropic barrier [30], and to the probability of the reaction event at each encounter [31, 32]. The interplay between diffusive transport from the bulk and reaction on the surface is controlled by the ratio  $q = \kappa/D$ , ranging from 0 for an inert boundary, to infinity for a perfectly reactive boundary. The inverse of  $q$ ,  $1/q$ , sets a characteristic reaction length [11, 19, 20, 31]. As the surface reaction mechanism is incorporated via the boundary condition (1), the dependence of the propagator  $G_q(\mathbf{x}, t|\mathbf{x}_0)$  on the reactivity  $\kappa$  (or  $q$ ) is *implicit* that impedes studying these phenomena and optimizing shapes and reactivity patterns of catalysts or clustering of receptors/pores on the cell membrane.

In this letter, we advocate for an alternative description of diffusion-mediated surface phenomena based on the concept of boundary local time. The main text describes our findings in a general and broadly accessible but still rigorous way (with a limited number of formulas), whereas the Supplemental Material (SM) provides all the necessary details for theoreticians. We recall that reflected Brownian motion  $\mathbf{X}_t$  in a confining domain  $\Omega \subset \mathbb{R}^d$  with a smooth *inert* boundary  $\partial\Omega$  is mathematically constructed as the solution of the stochastic Skorokhod equation [33–35]:

$$d\mathbf{X}_t = \sqrt{2D} d\mathbf{W}_t + \mathbf{n}(\mathbf{X}_t) d\ell_t, \quad \mathbf{X}_0 = \mathbf{x}_0, \quad (2)$$

where  $\mathbf{W}_t$  is the standard Brownian motion,  $\mathbf{n}(\mathbf{x})$  is the unit normal vector, and  $\ell_t$  (with  $\ell_0 = 0$ ) is a nondecreasing process, which increases only when  $\mathbf{X}_t \in \partial\Omega$ , known as the boundary local time (see Sec. SM.I of the SM for a discussion of this concept). Qualitatively, Eq. (2) can be understood as a Langevin equation with a very strong short-range repulsive force localized on the boundary. Indeed, the second term in Eq. (2) is nonzero only for  $\mathbf{X}_t \in \partial\Omega$  and ensures that the particle is reflected in the perpendicular direction  $\mathbf{n}(\mathbf{x})$  from the boundary at each encounter. The peculiar feature of this construction is that the single Skorokhod equation determines simultaneously two tightly related stochastic processes:  $\mathbf{X}_t$  and  $\ell_t$ . The conventional propagator  $G_0(\mathbf{x}, t|\mathbf{x}_0)$  (with  $q = 0$ ) characterizes the position  $\mathbf{X}_t$  of the diffusing particle but ignores its boundary local time  $\ell_t$ . But it is precisely the local time that bears information on particle’s encounters with the boundary and is thus the key ingredient to account for surface reactions. We therefore build an alternative description on the full propagator  $P(\mathbf{x}, \ell, t|\mathbf{x}_0)$ , i.e., the joint probability density of both  $\mathbf{X}_t$  and  $\ell_t$  at time  $t$ . Due to the jump-like character of the boundary local time (see Fig. 1(b)), finding the full propagator was the most challenging and mathematically involved part of this work (see Sec. SM.II).

As the full propagator characterizes the diffusive dynamics alone (without reactions), it is the most natural theoretical ground, to which both bulk and surface reactions can be added *explicitly* via stopping conditions. Indeed, if the diffusing particle can spontaneously die,

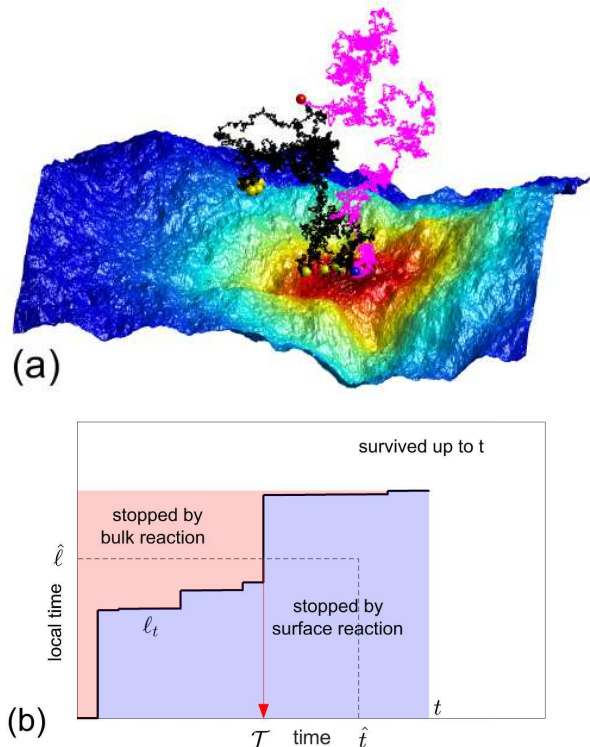


FIG. 1: (a) A simulated trajectory of a particle diffusing over a reactive surface (see SM.VIII for details). Red, blue and yellow balls indicate respectively the starting bulk point  $\mathbf{x}_0$ , the first arrival point  $\mathbf{s}_0$  onto the surface, the consequent boundary points at which the particle encountered the surface. Pink and black colors encode respectively the first segment of the trajectory (from red to blue ball), and the remaining part. (b) The boundary local time  $\ell_t$  of the simulated trajectory (black thick line). The statistics of  $\ell_t$  is determined by reflected Brownian motion, while bulk and surface reaction mechanisms are then incorporated by introducing a stopping time  $\hat{t}$  (vertical dashed line) and a stopping local time  $\hat{\ell}$  (horizontal dashed line), respectively. The surface reaction time  $\mathcal{T} = \inf\{t > 0 : \ell_t > \hat{\ell}\}$  is the random moment (indicated by arrow) when the boundary local time  $\ell_t$  crosses the horizontal line at  $\hat{\ell}$ .

relax its excitation, be chemically transformed, killed or destroyed in the bulk, its finite lifetime can be modeled by a random stopping time  $\hat{t}$ . In a common Poissonian setting, such a bulk reaction can occur at any time instance with equal chances (characterized by rate  $p$ ), so that the lifetime of the particle obeys the exponential distribution:  $\mathbb{P}\{\hat{t} > t\} = e^{-pt}$ . If this bulk reaction mechanism is independent of the diffusive dynamics, averaging the full propagator  $P(\mathbf{x}, \ell, \hat{t}|\mathbf{x}_0)$  over random realizations of  $\hat{t}$  yields the joint distribution of  $\mathbf{X}_{\hat{t}}$  and  $\ell_{\hat{t}}$  at the moment  $\hat{t}$  of bulk reaction (or particle’s death). More generally, one can introduce elaborate stopping times to incorporate eventual delays in the bulk diffusion due to reversible binding to immobile centers

or mobile buffer molecules (like waiting time distribution in continuous-time random walks), time-dependent or switching diffusivity, the effects of rapidly re-arranging dynamic medium, and other subordination mechanisms (see [37–39] and references therein).

Remarkably, we discovered that surface reaction mechanisms can be implemented in essentially the same way. At each encounter with the partially reactive surface, the particle either reacts with the probability  $\Pi = 1/(1 + D/(\kappa a)) \simeq aq \ll 1$ , or resumes its bulk diffusion with the probability  $1 - \Pi$ , where  $a$  is the width of a thin reactive boundary layer (i.e., the interaction range) [31]. If all reaction attempts are independent from each other, the number  $\hat{n}$  of failed attempts until the successful reaction follows the geometric law,  $\mathbb{P}\{\hat{n} > n\} = (1 - \Pi)^n \approx \exp(-qna)$ . The rescaled number of failed reaction attempts,  $\hat{\ell} = a\hat{n}$ , obeys thus the exponential law:  $\mathbb{P}\{\hat{\ell} > \ell\} = e^{-q\ell}$ , with  $\ell = an$ . As the boundary local time  $\ell_t$  is related to the number  $\mathcal{N}_t^a$  of encounters of the particle with the surface up to time  $t$ ,  $\ell_t = \lim_{a \rightarrow 0} a\mathcal{N}_t^a$  [33, 34] (see also SM.I), the reaction time  $\mathcal{T}$  can be defined as the moment, at which  $\ell_t$  exceeds an independent random stopping local time  $\hat{\ell}$ :  $\mathcal{T} = \inf\{t > 0 : \ell_t > \hat{\ell}\}$  [32, 40, 41]. Multiplication of the full propagator  $P(\mathbf{x}, \ell, t|\mathbf{x}_0)$  by the probability  $\mathbb{P}\{\hat{\ell} > \ell\} = e^{-q\ell}$  of no surface reaction up to  $\ell$  and integration over  $\ell$  yield the marginal propagator of the position  $\mathbf{X}_t$  at time  $t$  of a particle, conditioned to survive up to time  $t$  (i.e., with the condition  $\mathcal{T} > t$ , which is equivalent to  $\hat{\ell} > \ell_t$ ). By construction, this average is precisely the conventional propagator:

$$G_q(\mathbf{x}, t|\mathbf{x}_0) = \int_0^\infty d\ell e^{-q\ell} P(\mathbf{x}, \ell, t|\mathbf{x}_0). \quad (3)$$

To our knowledge, this fundamental relation was not reported earlier.

Moreover, changing the distribution of the stopping local time  $\hat{\ell}$ , one can now easily implement new surface reaction mechanisms. In fact, the average of the full propagator  $P(\mathbf{x}, \ell, t|\mathbf{x}_0)$  with the probability of no surface reaction up to  $\ell$ , now determined by a desired distribution  $\Psi(\ell) = \mathbb{P}\{\hat{\ell} > \ell\}$  of  $\hat{\ell}$ , yields a generalized propagator

$$G_\psi(\mathbf{x}, t|\mathbf{x}_0) = \int_0^\infty d\ell \Psi(\ell) P(\mathbf{x}, \ell, t|\mathbf{x}_0). \quad (4)$$

This relation couples explicitly the surface reaction mechanism (represented by  $\Psi(\ell)$ ) and the dynamics of the particle diffusing in a domain with reflecting boundary (represented by  $P(\mathbf{x}, \ell, t|\mathbf{x}_0)$ ). The striking similarity of our implementations of bulk and surface reactions is not surprising: while time  $t$  mimics the number of bulk steps (and thus exposure of the particle to bulk reaction), the local time  $\ell$  counts the number of encounters with the boundary (and its exposure to surface reaction). It is

crucial that both bulk and surface reaction mechanisms, introduced via two independent random variables  $\hat{t}$  and  $\hat{\ell}$  (Fig. 1(b)), are disentangled from the dynamics. In other words, one can first investigate the dynamics in the case of reflecting boundary and then couple it explicitly to reaction mechanisms.

The alternative description allows one to go far beyond the constant reactivity based on the Robin boundary condition (1). Indeed, the former exponential law  $\Psi(\ell) = e^{-q\ell}$  described a Poissonian-like mechanism when the particle could react at each encounter with the boundary with equal probabilities. To incorporate variable reaction probabilities, we introduce the reactivity  $\kappa(\ell)$  that changes with the local time  $\ell$  (i.e., with the rescaled number of encounters), alike time-dependent diffusivity  $D(t)$  for bulk diffusion. Extending our previous arguments (see SM.III), we derive the probability distribution for the corresponding stopping local time  $\hat{\ell}$ :

$$\Psi(\ell) = \exp\left(-\frac{1}{D} \int_0^\ell d\ell' \kappa(\ell')\right). \quad (5)$$

This is a new feature brought by our probabilistic description, which allows us to investigate within the unique theoretical framework many important diffusion-mediated surface phenomena such as catalyst's fooling or membrane degradation [42, 43]. In fact, choosing an appropriate  $\kappa(\ell)$  (or  $\Psi(\ell)$ ), one can control the reaction dynamics of the boundary. For instance, the reactivity  $\kappa(\ell)$ , which is small at  $\ell \approx 0$  and then reaches a constant level, can model situations when the surface needs to be progressively activated by repeated encounters with the diffusing particle. In contrast, when  $\kappa(\ell)$  is large at small  $\ell$  and then reaches a constant (or vanishes), one models a progressive passivation of initially highly reactive surfaces.

The generalized propagator  $G_\psi(\mathbf{x}, t|\mathbf{x}_0)$  determines other common characteristics of diffusion-reaction processes such as, e.g., the survival probability or the reaction rate (see Fig. S2 and SM.IV). For instance, we show in the SM that the probability density of the first-passage (or reaction) time  $\mathcal{T}$  can be written as

$$H_\psi(t|\mathbf{x}_0) = \int_0^\infty d\ell \psi(\ell) U(\ell, t|\mathbf{x}_0), \quad (6)$$

where  $\psi(\ell) = -d\Psi(\ell)/d\ell$  is the probability density of the stopping local time  $\hat{\ell}$ , and  $U(\ell, t|\mathbf{x}_0) = D \int_{\partial\Omega} d\mathbf{s} P(\mathbf{s}, \ell, t|\mathbf{x}_0)$  is the probability density of the first-crossing time of a level  $\ell$  by the boundary local time  $\ell_t$  (see SM.IIF). This relation expresses the idea illustrated in Fig. 1(b): the surface reaction occurs when the boundary local time  $\ell_t$  exceeds a random level  $\hat{\ell}$  determined by  $\psi(\ell)$ . For a perfectly reactive boundary, the reaction occurs at the first encounter with the boundary, i.e., at the first moment when the boundary local time exceeds 0. This is precisely the first-crossing time

of the level 0, i.e.,  $\psi(\ell) = \delta(\ell)$ , and thus  $U(0, t|\mathbf{x}_0)$  is the probability density of the common first-passage time to a perfect target [44]. In turn,  $U(\ell, t|\mathbf{x}_0)$  for any  $\ell > 0$  describes the reaction time in the case when the reaction occurs at the boundary local time  $\ell_t = \ell$  (i.e., after a prescribed number of failed reaction attempts). According to Eq. (6), other surface reaction mechanisms can be described by setting the level  $\ell$  randomly, i.e., by introducing the stopping local time  $\hat{\ell}$ .

Figure 2 exemplifies the impact of surface reaction mechanisms onto the distribution of the reaction time. Here the family of the probability densities  $U(\ell, t|\mathbf{x}_0)$  (parameterized by  $\ell$ ) is presented for a spherical target, surrounded by an outer reflecting sphere. Three probability densities  $\psi(\ell)$  determining surface reaction mechanisms (with  $\kappa(\ell)$  in the inset) are plotted on the left projection, while the resulting reaction time densities  $H_\psi(t|\mathbf{x}_0)$  are shown on the right projection. For a constant reactivity, the average of  $U(\ell, t|\mathbf{x}_0)$  with the exponential density  $qe^{-q\ell}$  (gray line) results in the conventional reaction time distribution [45]. Here, a single ‘‘hump’’ region around the most probable reaction time is followed by a flat part and ultimate exponential decay, as it should be for a bounded domain. If the target is passive at the beginning (red line), first arrivals of the particle onto the target do not produce reaction up to some local time  $\ell_0$ , thus shifting the probability density of the reaction time to longer times. Curiously, an unusual second ‘‘hump’’ region emerges due to the particles that moved away from the target, explored the confining domain and then returned to the target (see also SM.VI). In the third example (blue line), the reactivity is negligible at the beginning, reaches a maximum around  $\ell/R \approx 0.7$ , and then slowly decreases as  $1/(2q\ell)$  at large  $\ell$ . The overall shape of the reaction time density  $H_\psi(t|\mathbf{x}_0)$  resembles that of the conventional setting, but exhibits anomalous power law decay at long times:  $H_\psi(t|\mathbf{x}_0) \propto t^{-3/2}$ . Here, as the encounter-dependent reactivity offers an optimal range of local times for surface reaction, a particle that failed to react during this range, has lower and lower chances to react after more or more returns to the target.

More generally, the asymptotic large- $\ell$  decay  $\kappa(\ell) \propto 1/\ell$  turns out to be the critical regime that distinguished three scenarios for arbitrary bounded domains (see SM.VI): (i) if  $\kappa(\ell)$  decays slower than  $1/\ell$  (or increases with  $\ell$ ),  $H_\psi(t|\mathbf{x}_0)$  exhibits the long-time exponential decay, as in the conventional setting; (ii) if  $\kappa(\ell)$  decreases as  $\nu D/\ell$  with some constant  $0 < \nu < 1$ , then  $H_\psi(t|\mathbf{x}_0) \propto t^{-1-\nu}$ ; this is a new unexpected feature for bounded domains; (iii) if  $\kappa(\ell)$  decays faster than  $1/\ell$ , the reaction time can be infinite with a finite probability:

$$\mathbb{P}\{\mathcal{T} = \infty\} = \Psi(\infty) = \exp\left(-\int_0^\infty d\ell \frac{\kappa(\ell)}{D}\right) > 0. \quad (7)$$

In other words, this is the probability of no surface reaction in a bounded domain: even though the exploration is compact, the reactivity decays too fast so that the

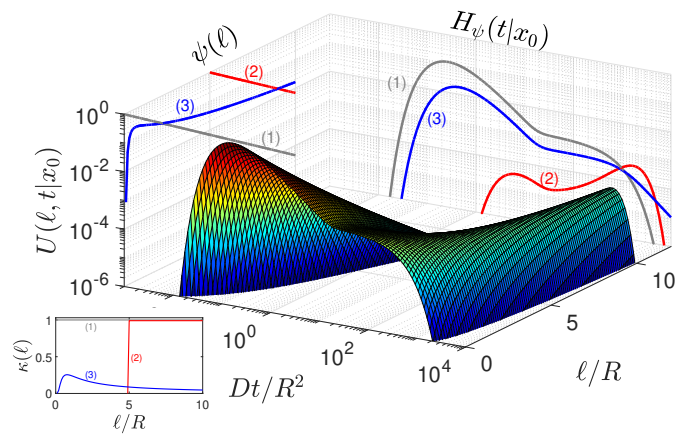


FIG. 2: The probability density  $U(\ell, t|\mathbf{x}_0)$  (rescaled by  $R^2/D$ ) of the first-crossing time of a level  $\ell$  by the boundary local time  $\ell_t$  for a spherical target of radius  $R$ , surrounded by an outer reflecting concentric sphere of radius  $L$ , with  $|\mathbf{x}_0|/R = 2$  and  $L/R = 10$ . Three curves on the left projection illustrate three probability densities  $\psi(\ell)$  of the stopping local time  $\hat{\ell}$  (with  $qR = 1$ ): (1)  $\psi(\ell) = qe^{-q\ell}$  (gray line, conventional setting); (2)  $\psi(\ell) = qe^{-q\ell}\Theta(\ell - \ell_0)$  with  $\ell_0/R = 5$  (red line); and (3)  $\psi(\ell) = qe^{-1/(q\ell)}/[\sqrt{\pi}(q\ell)^{3/2}]$  (blue line). These densities correspond respectively to three reactivity profiles shown on the inset:  $\kappa(\ell) = qD$ ,  $\kappa(\ell) = qD\Theta(\ell - \ell_0)$ , and  $\kappa(\ell) = qDe^{-1/(q\ell)}/[\sqrt{\pi}(q\ell)^{3/2}\text{erf}(1/\sqrt{q\ell})]$ . Three curves on the right projection show the corresponding probability densities  $H_\psi(t|\mathbf{x}_0)$  from Eq. (6).

particle may fail to react even after an infinite number of returns to the target. Several surface reaction models and the behavior of the underlying reaction time distributions and reaction rates are discussed in SM.VI.

In summary, we developed a new probabilistic description of diffusion-mediated surface phenomena based on the concept of boundary local time. By introducing the full propagator to describe confined diffusion with reflections on the boundary, we succeeded to incorporate surface reactivity *explicitly* via a stopping condition. The disentanglement of the surface reactivity from the dynamics allowed us to introduce encounter-dependent reactivity  $\kappa(\ell)$  and to describe a variety of new surface reaction mechanisms. We discussed how different forms of  $\kappa(\ell)$  affect the reaction times and revealed some intriguing anomalous features in their distribution.

The developed formalism opens a vast area for future research. On the theoretical side, one can study how the diffusive dynamics in domains with complex geometric structures (such as the interior of an eukaryotic cell, a chemical reactor, or a human acinus) is coupled to different surface reaction mechanisms. One can further extend this approach to investigate (i) the (anti-)cooperativity effects of multiple diffusing particles whose individual encounters with the boundary change its reactivity; (ii) the competition between multiple targets, each described by its own boundary local time; (iii) the combined impact of

bulk and surface reaction mechanisms; (iv) the effects of correlations between successive encounters, and (v) the presence of long-range interactions with and reversible binding to the boundary. In particular, our probabilistic description of the bulk exploration step until reversible binding to the boundary can bring complementary insights to former theoretical approaches based on coupled diffusion-reaction equations [46, 47] (see SM.VII). On the application side, appropriate surface reaction models should be identified to describe industrial examples of catalyst fooling, membrane aging and many other

diffusion-mediated surface phenomena, in which the surface properties depend on the number of encounters. One can also address a new class of optimization problems targeting optimal reaction rates or prescribed distributions of reaction times or positions, either by adapting the surface reaction mechanisms for a given geometric structure of the medium, or by optimizing its structure for a given surface reaction mechanism, or both. The disentanglement of the geometric structure from the surface reaction mechanism is the key that has now opened the door to such applications.

- 
- [1] S. Rice, *Diffusion-Limited Reactions* (Elsevier, Amsterdam, 1985).
- [2] S. Redner, *A Guide to First Passage Processes* (Cambridge: Cambridge University press, 2001).
- [3] Z. Schuss, *Brownian Dynamics at Boundaries and Interfaces in Physics, Chemistry and Biology* (Springer, New York, 2013).
- [4] R. Metzler, G. Oshanin, and S. Redner (Eds.) *First-Passage Phenomena and Their Applications* (Singapore: World Scientific, 2014).
- [5] K. Lindenberg, R. Metzler, and G. Oshanin (Eds.) *Chemical Kinetics: Beyond the Textbook* (New Jersey: World Scientific, 2019).
- [6] D. S. Grebenkov, “NMR Survey of Reflected Brownian Motion”, *Rev. Mod. Phys.* **79**, 1077-1137 (2007).
- [7] P. C. Bressloff and J. M. Newby, “Stochastic models of intracellular transport”, *Rev. Mod. Phys.* **85**, 135-196 (2013).
- [8] O. Bénichou and R. Voituriez, “From first-passage times of random walks in confinement to geometry-controlled kinetics”, *Phys. Rep.* **539**, 225-284 (2014).
- [9] O. V. Bychuk and B. O’Shaughnessy, “Anomalous Diffusion at Liquid Surfaces”, *Phys. Rev. Lett.* **74**, 1795 (1995).
- [10] D. Wang, H. Wu, and D. K. Schwartz, “Three-Dimensional Tracking of Interfacial Hopping Diffusion”, *Phys. Rev. Lett.* **119**, 268001 (2017).
- [11] B. Sapoval, M. Filoche, and E. Weibel, “Smaller is better – but not too small: A physical scale for the design of the mammalian pulmonary acinus”, *Proc. Nat. Ac. Sci. USA* **99**, 10411-10416 (2002).
- [12] D. S. Grebenkov, M. Filoche, B. Sapoval, and M. Felici, “Diffusion-Reaction in Branched Structures: Theory and Application to the Lung Acinus”, *Phys. Rev. Lett.* **94**, 050602 (2005).
- [13] A. S. Serov, C. Salafia, D. S. Grebenkov, and M. Filoche, “The Role of Morphology in Mathematical Models of Placental Gas Exchange”, *J. Appl. Physiol.* **120**, 17-28 (2016).
- [14] S. B. Yuste, E. Abad, and K. Lindenberg, “Exploration and trapping of mortal random walkers”, *Phys. Rev. Lett.* **110**, 220603 (2013).
- [15] B. Meerson and S. Redner, “Mortality, redundancy, and diversity in stochastic search”, *Phys. Rev. Lett.* **114**, 198101 (2015).
- [16] D. S. Grebenkov and J.-F. Rupprecht, “The escape problem for mortal walkers”, *J. Chem. Phys.* **146**, 084106 (2017).
- [17] H. Risken, *The Fokker-Planck equation: methods of solution and applications*, 3rd Ed. (Berlin: Springer, 1996).
- [18] F. C. Collins and G. E. Kimball, “Diffusion-controlled reaction rates”, *J. Coll. Sci.* **4**, 425 (1949).
- [19] B. Sapoval, “General Formulation of Laplacian Transfer Across Irregular Surfaces”, *Phys. Rev. Lett.* **73**, 3314-3317 (1994).
- [20] D. S. Grebenkov, M. Filoche, and B. Sapoval, “Mathematical Basis for a General Theory of Laplacian Transport towards Irregular Interfaces”, *Phys. Rev. E* **73**, 021103 (2006).
- [21] D. A. Lauffenburger and J. Linderman, *Receptors: Models for Binding, Trafficking, and Signaling* (Oxford University Press, 1993).
- [22] H. Sano and M. Tachiya, “Partially diffusion-controlled recombination”, *J. Chem. Phys.* **71**, 1276-1282 (1979).
- [23] D. Shoup and A. Szabo, “Role of diffusion in ligand binding to macromolecules and cell-bound receptors”, *Biophys. J.* **40**, 33-39 (1982).
- [24] R. Zwanzig, “Diffusion-controlled ligand binding to spheres partially covered by receptors: an effective medium treatment”, *Proc. Natl. Acad. Sci. USA* **87**, 5856 (1990).
- [25] A. Berezhkovskii, Y. Makhnovskii, M. Monine, V. Zitserman, and S. Shvartsman, “Boundary homogenization for trapping by patchy surfaces”, *J. Chem. Phys.* **121**, 11390 (2004).
- [26] A. Bernoff, A. Lindsay, and D. Schmidt, “Boundary Homogenization and Capture Time Distributions of Semipermeable Membranes with Periodic Patterns of Reactive Sites”, *Multiscale Model. Simul.* **16**, 1411-1447 (2018).
- [27] D. S. Grebenkov, “Spectral theory of imperfect diffusion-controlled reactions on heterogeneous catalytic surfaces”, *J. Chem. Phys.* **151**, 104108 (2019).
- [28] O. Bénichou, M. Moreau, and G. Oshanin, “Kinetics of stochastically gated diffusion-limited reactions and geometry of random walk trajectories”, *Phys. Rev. E* **61**, 3388-3406 (2000).
- [29] J. Reingruber and D. Holcman, “Gated Narrow Escape Time for Molecular Signaling”, *Phys. Rev. Lett.* **103**, 148102 (2009).
- [30] D. S. Grebenkov and G. Oshanin, “Diffusive escape through a narrow opening: new insights into a classic problem,” *Phys. Chem. Chem. Phys.* **19**, 2723-2739 (2017).

- [31] D. S. Grebenkov, M. Filoche, and B. Sapoval, “Spectral Properties of the Brownian Self-Transport Operator”, *Eur. Phys. J. B* **36**, 221-231 (2003).
- [32] D. S. Grebenkov, *Partially Reflected Brownian Motion: A Stochastic Approach to Transport Phenomena*, in “Focus on Probability Theory”, Ed. L. R. Velle, pp. 135-169 (Nova Science Publishers, 2006).
- [33] K. Ito and H. P. McKean, *Diffusion Processes and Their Sample Paths* (Springer-Verlag, Berlin, 1965).
- [34] M. Freidlin, *Functional Integration and Partial Differential Equations* (Annals of Mathematics Studies, Princeton University Press, Princeton, New Jersey, 1985).
- [35] Y. Saisho, “Stochastic Differential Equations for Multi-Dimensional Domain with Reflecting Boundary”, *Probab. Theory Rel. Fields* **74**, 455-477 (1987).
- [36] C. W. Gardiner, *Handbook of stochastic methods for physics, chemistry and the natural sciences* (Springer: Berlin, 1985).
- [37] R. Metzler and J. Klafter, “The random walk’s guide to anomalous diffusion: a fractional dynamics approach”, *Phys. Rev.* **339**, 1-77 (2000).
- [38] A. V. Chechkin, F. Seno, R. Metzler, and I. M. Sokolov, “Brownian yet Non-Gaussian Diffusion: From Superstatistics to Subordination of Diffusing Diffusivities”, *Phys. Rev. X* **7**, 021002 (2017).
- [39] Y. Lanoiselée, N. Moutal, and D. S. Grebenkov, “Diffusion-limited reactions in dynamic heterogeneous media”, *Nat. Commun.* **9**, 4398 (2018).
- [40] D. S. Grebenkov, “Residence times and other functionals of reflected Brownian motion”, *Phys. Rev. E* **76**, 041139 (2007);
- [41] D. S. Grebenkov, “Probability distribution of the boundary local time of reflected Brownian motion in Euclidean domains”, *Phys. Rev. E* **100**, 062110 (2019).
- [42] C. H. Bartholomew, “Mechanisms of catalyst deactivation”, *Appl. Catal. A: Gen.* **212**, 17-60 (2001).
- [43] M. Filoche, D. S. Grebenkov, J. S. Andrade Jr., and B. Sapoval, “Passivation of Irregular Surfaces Accessed by Diffusion”, *Proc. Natl. Acad. Sci.* **105**, 7636-7640 (2008).
- [44] O. Bénichou, C. Chevalier, J. Klafter, B. Meyer, and R. Voituriez, “Geometry-controlled kinetics”, *Nature Chem.* **2**, 472-477 (2010).
- [45] D. S. Grebenkov, R. Metzler, and G. Oshanin, “Strong defocusing of molecular reaction times results from an interplay of geometry and reaction control”, *Commun. Chem.* **1**, 96 (2018).
- [46] A. V. Chechkin, I. M. Zaid, M. Lomholt, I. M. Sokolov, and R. Metzler, “Bulk-mediated surface diffusion along a cylinder: Propagators and crossovers”, *Phys. Rev. E* **79**, 040105(R) (2009).
- [47] A. M. Berezhkovskii, L. Dagdug, and S. M. Bezrukov, “A new approach to the problem of bulk-mediated surface diffusion”, *J. Chem. Phys.* **143**, 084103 (2015).
- [48] P. Lévy, *Processus Stochastiques et Mouvement Brownien* (Paris, Gauthier-Villard, 1965).
- [49] A. N. Borodin and P. Salminen, *Handbook of Brownian Motion: Facts and Formulae* (Birkhauser Verlag, Basel-Boston-Berlin, 1996).
- [50] E. Hsu, “Probabilistic approach to the Neumann problem”, *Comm. Pure Appl. Math.* **38**, 445-472 (1985).
- [51] R. J. Williams, “Local Time and Excursions of Reflected Brownian Motion in a Wedge”, *Publ. RIMS* **23**, 297-319 (1987).
- [52] L. Takacs, “On the Local Time of the Brownian Motion”, *Ann. Appl. Probab.* **5**, 741-756 (1995).
- [53] Y. Zhou, W. Cai, and E. Hsu, “Computation of the local time of reflecting Brownian motion and the probabilistic representation of the Neumann problem”, *Comm. Math. Sci.* **15**, 237-259 (2017).
- [54] P. Mörters and Y. Peres, *Brownian Motion* (Cambridge Series in Statistical and Probabilistic Mathematics, Cambridge University Press, Cambridge, 2010).
- [55] D. S. Grebenkov, “Imperfect Diffusion-Controlled Reactions”, in *Chemical Kinetics: Beyond the Textbook*, Eds. K. Lindenberg, R. Metzler, and G. Oshanin (World Scientific, 2019).
- [56] V. G. Papanicolaou, “The probabilistic solution of the third boundary value problem for second order elliptic equations”, *Probab. Th. Rel. Fields* **87**, 27-77 (1990).
- [57] R. F. Bass, K. Burdzy, and Z.-Q. Chen, “On the Robin problem in Fractal Domains”, *Proc. London Math. Soc.* **96**, 273-311 (2008).
- [58] M. Filoche and B. Sapoval, “Can One Hear the Shape of an Electrode? II. Theoretical Study of the Laplacian Transfer”, *Eur. Phys. J. B* **9**, 755-763 (1999).
- [59] W. Arendt, A. F. M. ter Elst, J. B. Kennedy, and M. Sauter, “The Dirichlet-to-Neumann operator via hidden compactness”, *J. Funct. Anal.* **266**, 1757-1786 (2014).
- [60] D. Daners, “Non-positivity of the semigroup generated by the Dirichlet-to-Neumann operator”, *Positivity* **18**, 235-256 (2014).
- [61] W. Arendt and A. F. M. ter Elst, “The Dirichlet-to-Neumann Operator on Exterior Domains”, *Potential Anal.* **43**, 313-340 (2015).
- [62] A. Hassell and V. Ivrii, “Spectral asymptotics for the semiclassical Dirichlet to Neumann operator”, *J. Spectr. Theory* **7**, 881-905 (2017).
- [63] A. Girouard and I. Polterovich, “Spectral geometry of the Steklov problem”, *J. Spectr. Theory* **7**, 321-359 (2017).
- [64] G. Wilemski and M. Fixman, “General theory of diffusion-controlled reactions”, *J. Chem. Phys.* **58**, 4009 (1973).
- [65] X. Li, J. Lowengrub, A. Rätz, and A. Voigt, “Solving PDEs in complex geometries: a diffusion domain approach”, *Commun. Math. Sci.* **7**, 81-107 (2009).
- [66] H.-C. Yu, H.-Y. Chen, and K. Thornton, “Extended smoothed boundary method for solving partial differential equations with general boundary conditions on complex boundaries”, *Model Simul Mater. Sci. Eng.* **20**, 075008 (2012).
- [67] D. S. Grebenkov, “Scaling Properties of the Spread Harmonic Measures”, *Fractals* **14**, 231-243 (2006).
- [68] D. S. Grebenkov, “Analytical representations of the spread harmonic measure density”, *Phys. Rev. E* **91**, 052108 (2015).
- [69] D. S. Grebenkov, “A physicist’s guide to explicit summation formulas involving zeros of Bessel functions and related spectral sums” (submitted; available online arXiv:1904.11190v2)
- [70] M. Smoluchowski, “Versuch einer Mathematischen Theorie der Koagulations Kinetik Kolloider Lösungen”, *Z. Phys. Chem.* **129**, 129-168 (1917).
- [71] D. S. Grebenkov, “Subdiffusion in a bounded domain with a partially absorbing-reflecting boundary”, *Phys. Rev. E* **81**, 021128 (2010).
- [72] A. V. Chechkin, I. M. Zaid, M. Lomholt, I. M. Sokolov, and R. Metzler, “Effective surface motion on a reactive cylinder of particles that perform intermittent bulk dif-

- fusion”, *J. Chem. Phys.* **134**, 204116 (2011).
- [73] A. V. Chechkin, I. M. Zaid, M. Lomholt, I. M. Sokolov, and R. Metzler, “Bulk-mediated diffusion on a planar surface: Full solution”, *Phys. Rev. E* **86**, 041101 (2012).
- [74] A. M. Berezhkovskii, L. Dagdug, and S. M. Bezrukov, “Bulk-mediated surface transport in the presence of bias”, *J. Chem. Phys.* **147**, 014103 (2017).
- [75] O. G. Berg, R. B. Winter, and P. H. von Hippel, “Diffusion-driven mechanisms of protein translocation on nucleic acids. 1. Models and theory”, *Biochemistry* **20**, 6929-6948 (1981).
- [76] N. Agmon and A. Szabo, “Theory of reversible diffusion-influenced reactions,” *J. Chem. Phys.* **92**, 5270 (1990).
- [77] T. Prüstel and M. Tachiya, “Reversible diffusion-influenced reactions of an isolated pair on some two dimensional surfaces”, *J. Chem. Phys.* **139**, 194103 (2013).
- [78] O. Bénichou, D. S. Grebenkov, P. Levitz, C. Loverdo, and R. Voituriez, “Optimal Reaction Time for Surface-Mediated Diffusion”, *Phys. Rev. Lett.* **105**, 150606 (2010).
- [79] O. Bénichou, D. S. Grebenkov, P. Levitz, C. Loverdo, and R. Voituriez, “Mean First-Passage Time of Surface-Mediated Diffusion in Spherical Domains”, *J. Stat. Phys.* **142**, 657-685 (2011).
- [80] F. Rojo and C. E. Budde, “Enhanced diffusion through surface excursion: A master-equation approach to the narrow-escape-time problem”, *Phys. Rev. E* **84**, 021117 (2011).
- [81] J.-F. Rupprecht, O. Bénichou, D. S. Grebenkov, and R. Voituriez, “Kinetics of Active Surface-Mediated Diffusion in Spherically Symmetric Domains”, *J. Stat. Phys.* **147**, 891-918 (2012).
- [82] J.-F. Rupprecht, O. Bénichou, D. S. Grebenkov, and R. Voituriez, “Exact mean exit time for surface-mediated diffusion”, *Phys. Rev. E* **86**, 041135 (2012).
- [83] F. Rojo, C. E. Budde Jr., H. S. Wio, and C. E. Budde, “Enhanced transport through desorption-mediated diffusion”, *Phys. Rev. E* **87**, 012115 (2013).
- [84] M. M. Kanafi, “Surface generator: artificial randomly rough surfaces” (n. 60817), MATLAB Central File Exchange. Retrieved September 29, 2019.

SUPPLEMENTAL MATERIAL

Contents

<b>SM.I. Boundary local time</b>	8
<b>SM.II. Derivation of main results</b>	10
A. Full propagator	10
B. Surface hopping propagator	12
C. Dirichlet-to-Neumann operator	13
D. Boundary value problem for the full propagator	14
E. Distribution of the boundary local time	15
F. Distribution of the first-crossing time	16
<b>SM.III. Encounter-dependent reactivity</b>	16
<b>SM.IV. Generalized quantities</b>	17
<b>SM.V. Spherical shell</b>	19
<b>SM.VI. Surface reaction models</b>	20
A. Selected models	20
B. Reaction rate on a spherical target	20
C. Distribution of the reaction time	22
<b>SM.VII. Comparison with bulk-mediated surface diffusion</b>	23
<b>SM.VIII. Description of figure 1</b>	24

SM.I. BOUNDARY LOCAL TIME

While the boundary local time is a cornerstone of the mathematical theory of stochastic processes [33, 34], this important classic concept remains largely unknown in physical, chemical and biological communities. As the boundary local time plays the central role in our probabilistic description of diffusion-mediated surface phenomena, we provide here a short introduction for physicists.

The notion of a (point) local time has been first introduced by Lévy to quantify a fraction of time that Brownian motion spent at that point [48]. The properties of point local times were thoroughly investigated, in particular, for Brownian motion and Bessel processes (see [49] and references therein). This notion was extended to boundaries and applied for a rigorous mathematical construction of diffusive processes that are confined inside a given domain  $\Omega$  with a smooth boundary  $\partial\Omega$  [33, 34]. The distribution of the boundary local time for some Euclidean domains was investigated [40, 41] (see also [50–53]) and will also be discussed in Sec. SM.II E.

To get an intuitive feeling of this construction, let us consider the Langevin equation for a particle diffusing in

a force field  $\mathbf{F}(\mathbf{x})$ :

$$d\mathbf{X}_t = \frac{D}{k_B T} \mathbf{F}(\mathbf{X}_t) dt + \sqrt{2D} d\mathbf{W}_t, \quad (\text{S1})$$

where  $\mathbf{W}_t$  is the standard Brownian motion (representing the thermally induced motion),  $D$  is the diffusion coefficient, and  $D/(k_B T)$  is the drag coefficient related to the fluid viscosity (with  $k_B$  being the Boltzmann constant and  $T$  the absolute temperature). As Brownian motion  $\mathbf{W}_t$  can explore the whole Euclidean space, the force field is needed to keep the particle inside the domain  $\Omega$ . If one aims at constructing reflected Brownian motion (i.e., ordinary diffusion with reflections on  $\partial\Omega$ ), the force field should not affect the motion inside the domain. In other words,  $\mathbf{F}(\mathbf{x})$  should be zero inside  $\Omega$ , except for a very thin boundary layer of width  $a$ , in which  $\mathbf{F}(\mathbf{x})$  should force the particle to move away from the boundary back to the interior (a sort of repulsion). Moreover, as the force acts only in that thin layer, its repulsive action should be strong enough to avoid any crossing of the boundary. A simple choice of the force field is

$$\frac{\mathbf{F}(\mathbf{x})}{k_B T} = \frac{1}{a} \mathbf{n}(\mathbf{x}) \mathbb{I}_{\partial\Omega_a}(\mathbf{x}), \quad (\text{S2})$$

where  $\mathbf{n}(\mathbf{x})$  is the normal vector to the boundary  $\partial\Omega$  determining the force direction back to the bulk in the orthogonal direction (to avoid any longitudinal bias along the boundary),  $\partial\Omega_a = \{\mathbf{x} \in \Omega : |\mathbf{x} - \partial\Omega| < a\}$  is the boundary layer of width  $a$ , inside which the force acts, and  $\mathbb{I}_{\partial\Omega_a}(\mathbf{x})$  is the indicator function of  $\partial\Omega_a$ :  $\mathbb{I}_{\partial\Omega_a}(\mathbf{x}) = 1$  if  $\mathbf{x} \in \partial\Omega_a$  and 0 otherwise. The factor  $1/a$  increases the force amplitude when the layer width diminishes. Denoting

$$\ell_t^a = \frac{D}{a} \int_0^t dt' \mathbb{I}_{\partial\Omega_a}(\mathbf{X}_{t'}), \quad (\text{S3})$$

the Langevin equation takes the form

$$d\mathbf{X}_t = \mathbf{n}(\mathbf{X}_t) d\ell_t^a + \sqrt{2D} d\mathbf{W}_t. \quad (\text{S4})$$

By definition,  $(a/D)\ell_t^a$  is the residence (or occupation) time of the process  $\mathbf{X}_t$  inside the boundary layer  $\partial\Omega_a$  up to time  $t$ . As the boundary layer is getting thinner ( $a \rightarrow 0$ ), its volume and thus the residence time in  $\partial\Omega_a$  vanish. However, the rescaling by  $1/a$  ensures a nontrivial limit,

$$\ell_t = \lim_{a \rightarrow 0} \ell_t^a, \quad (\text{S5})$$

while the above Langevin equation yields the stochastic Skorokhod equation

$$d\mathbf{X}_t = \mathbf{n}(\mathbf{X}_t) d\ell_t + \sqrt{2D} d\mathbf{W}_t. \quad (\text{S6})$$

The stochastic process  $\ell_t$  is called the boundary local time. Even though  $\ell_t$  has units of length (due to the factor  $D/a$  in Eq. (S3)), it can still be thought of as a

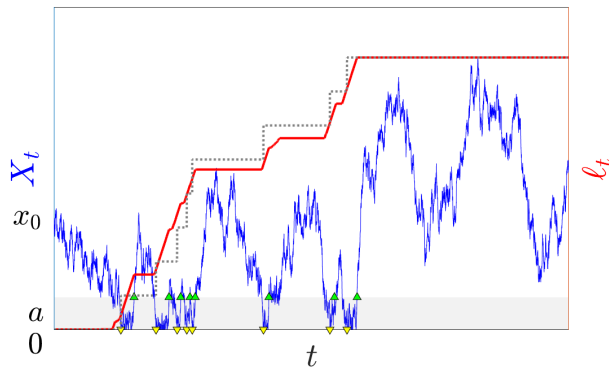


FIG. S1: Simulated random trajectory (blue line) of reflected Brownian motion  $X_t$  on the half-line  $\Omega = (0, \infty)$  (vertical axis) and two approximations  $\ell_t^a$  (red solid line) and  $a\mathcal{N}_t^a$  (gray dotted line) of the boundary local time  $\ell_t$  at the origin, all plotted as functions of time  $t$ . Shaded region outlines the zone when the particle diffuses inside the boundary layer  $\partial\Omega_a = (0, a)$  near the origin ( $\partial\Omega = \{0\}$ ). Yellow down-pointing triangles indicate the hitting times  $\delta_n^{(0)}$  when the particle downcrossed the boundary layer; in turn, green up-pointing triangles show the hitting times  $\delta_n^{(a)}$  when the particle left the boundary layer after crossing. Note that  $X_t$ ,  $\ell_t^a$  and  $a\mathcal{N}_t^a$  are rescaled to the same maximum for easier visualization.

fraction of time that reflected Brownian motion spent in an infinitesimal vicinity of the boundary up to time  $t$ . By construction, the first term in Eq. (S6) is nonzero only when  $\mathbf{X}_t$  is on the boundary (to highlight this property, the indicator function  $\mathbb{I}_{\partial\Omega}(\mathbf{X}_t)$  is sometimes included explicitly to the first term). We hasten to stress that this is not a rigorous derivation of the Skorokhod equation but rather its intuitive physical explanation.

The boundary local time  $\ell_t$  can also be related to the number  $\mathcal{N}_t^a$  of (down)crossings of the boundary layer  $\partial\Omega_a$  by reflected Brownian motion up to time  $t$ . This number can be defined by introducing a sequence of interlacing hitting times  $0 \leq \delta_1^{(0)} < \delta_1^{(a)} < \delta_2^{(0)} < \delta_2^{(a)} < \dots$  as

$$\delta_n^{(0)} = \inf\{t > \delta_{n-1}^{(a)} : \mathbf{X}_t \in \partial\Omega\}, \quad (\text{S7a})$$

$$\delta_n^{(a)} = \inf\{t > \delta_n^{(0)} : \mathbf{X}_t \in \Gamma_a\}, \quad (\text{S7b})$$

(with  $\delta_0^{(0)} = \delta_0^{(a)} = 0$ ), where  $\Gamma_a = \{\mathbf{x} \in \Omega : |\mathbf{x} - \partial\Omega| = a\}$  (see, e.g., [41]). Here, one records the first moment  $\delta_1^{(0)}$  when reflected Brownian motion hits the boundary  $\partial\Omega$ , then the first moment  $\delta_1^{(a)}$  of leaving the thin layer  $\partial\Omega_a$  through its inner boundary  $\Gamma_a$ , then the next moment  $\delta_2^{(0)}$  of hitting the boundary  $\partial\Omega$ , and so on. The number of downcrossings of the thin layer  $\partial\Omega_a$  up to time  $t$  is then the index  $n$  of the largest hitting time  $\delta_n^{(0)}$ , which is below  $t$ :

$$\mathcal{N}_t^a = \sup\{n \geq 0 : \delta_n^{(0)} < t\}. \quad (\text{S8})$$

While the number of downcrossings diverges as  $a \rightarrow 0$ , its rescaling by  $a$  yields the boundary local time [33, 34]:

$$\ell_t = \lim_{a \rightarrow 0} a\mathcal{N}_t^a. \quad (\text{S9})$$

As the number of encounters of the process  $\mathbf{X}_t$  with the boundary layer  $\partial\Omega_a$  up to time  $t$  can be naturally identified with the number  $\mathcal{N}_t^a$  of its downcrossings, the boundary local time divided by the layer width,  $\ell_t/a$ , is a proxy of the number of encounters, as soon as  $a$  is small enough. Note that the approximations  $a\mathcal{N}_t^a$  and  $\ell_t^a$  are closely related. Indeed, the residence time in Eq. (S3) can be split into separate contributions associated to each downcrossing, and each contribution is of the order  $a^2/D$  (the average time spent by reflected Brownian motion in a thin boundary layer  $\partial\Omega_a$ ).

By construction, the boundary local time  $\ell_t$  is a non-decreasing stochastic process, which remains 0 until the first encounter with the boundary. After that,  $\ell_t$  increases by tiny (infinitely small) jumps at every encounter with the boundary. These increments can also be interpreted as increases of the residence time spent near the boundary. In turn, the time interval between two successive jumps in  $\ell_t$  can be either small, or large. In fact, reflected Brownian motion hitting a smooth surface is known to return infinitely many times to that surface within an infinitely short time period [54]. Even if each of these returns gives a tiny increment to the boundary local time, their huge number results in notable changes of  $\ell_t$ . In contrast, when the particle diffuses inside the domain, the boundary local time remains constant until the next hit.

Figure S1 illustrates two approximations  $\ell_t^a$  and  $a\mathcal{N}_t^a$  of this process for reflected Brownian motion on a half-line. One can see that  $\ell_t^a$  increases gradually due to its integral form (S3), whereas  $a\mathcal{N}_t^a$  changes by jumps of height  $a$  at each downcrossing of the boundary layer. While these approximations behave quite differently for any finite  $a$ , both of them converge to the boundary local time  $\ell_t$  as  $a \rightarrow 0$ .

We conclude this section by highlighting some features of reflected Brownian motion  $\mathbf{X}_t$  and its boundary local time  $\ell_t$ . The contact of the diffusing particle with the reflecting boundary is instantaneous, the particle does not stay on that boundary as there is no binding. However, the self-similar nature of Brownian motion results in infinitely many returns of this process to the boundary whose accumulation yields nonzero increments in  $\ell_t$ . We stress that there is no attractive force to keep the particle close to the boundary, it is just a probabilistic consequence of white noise thermal fluctuations. If some of these properties may sound unphysical, it is because the mathematical processes  $\mathbf{X}_t$  and  $\ell_t$  are the limits of their “regularized”, more physically appealing versions (e.g., a random walk  $\mathbf{X}_t^a$  for  $\mathbf{X}_t$  and  $\ell_t^a$  or  $a\mathcal{N}_t^a$  for  $\ell_t$ ) when  $a \rightarrow 0$ . In a physical system, there is always a natural boundary layer (set, e.g., by atomic short-range interactions) so that one can keep thinking of  $\mathbf{X}_t$  and  $\ell_t$  in terms

of  $\mathbf{X}_t^a$  and  $\ell_t^a$  (or  $a\mathcal{N}_t^a$ ). Likewise, Monte Carlo techniques can only simulate “regularized” processes. However, the crucial advantage of the limiting processes  $\mathbf{X}_t$  and  $\ell_t$  is that they do not depend on the boundary layer width  $a$ , and their properties are thus more universal and in general easier to investigate by mathematical tools. Once these properties are established, one can use them to characterize systems with a small finite  $a$ .

## SM.II. DERIVATION OF MAIN RESULTS

In this section, we derive the main results of the letter. While this derivation employs and extends the arguments earlier developed [27, 41, 55], the probabilistic approach proposed in the letter and its major elements such as the full propagator, the generalized diffusion-reaction characteristics, and the encounter-dependent reactivity, are new. We hasten to stress that the following presentation does not provide mathematical proofs, so that its rigorous formulation and extensions present interesting perspectives for future work.

To facilitate reading, we summarize few basic notations:  $\mathbf{x}$  and  $\mathbf{x}_0$  are bulk points (in  $\bar{\Omega} = \Omega \cup \partial\Omega$ );  $\mathbf{s}$  and  $\mathbf{s}_0$  are boundary points (on  $\partial\Omega$ );  $\hat{t}$  and  $\hat{\ell}$  are random variables; tilde denotes the Laplace transform with respect to time  $t$  (see also Fig. S2 for notations of many other quantities). We also outline a slight abuse in notations for boundary points: in some functions,  $\mathbf{s}$  and  $\mathbf{s}_0$  are considered as points in  $\mathbb{R}^d$  lying on the boundary  $\partial\Omega$ ; in other formulas,  $\mathbf{s}$  and  $\mathbf{s}_0$  are understood as boundary points lying on a lower-dimensional manifold  $\partial\Omega$ . For instance, for a half-plane  $\mathbb{R} \times \mathbb{R}_+$ , the same notation will be used for a boundary point  $s \in \mathbb{R}$  and for a bulk point  $(s, 0) \in \mathbb{R}^2$  lying on the boundary. The dimensionality of such points clearly follows from the context; e.g., in Eq. (S27) below,  $G_q(\mathbf{s}, t|\mathbf{s}_0)$  is the bulk propagator with units  $\text{m}^{-d}$ , whereas  $\Sigma_p(\mathbf{s}, \ell|\mathbf{s}_0)$  is the surface hopping propagator with units  $\text{m}^{1-d}$ .

### A. Full propagator

The starting point of the conventional description is the propagator  $G_q(\mathbf{x}, t|\mathbf{x}_0)$  that characterizes the likelihood of finding a particle that started from a point  $\mathbf{x}_0$  at time 0 and not reacted up to time  $t$ , in a bulk point  $\mathbf{x}$  at time  $t$ . For ordinary diffusion in an Euclidean domain  $\Omega \subset \mathbb{R}^d$  with a smooth boundary  $\partial\Omega$ , the propagator satisfies the diffusion equation

$$\partial_t G_q(\mathbf{x}, t|\mathbf{x}_0) = D\Delta G_q(\mathbf{x}, t|\mathbf{x}_0) \quad (\mathbf{x} \in \Omega) \quad (\text{S10})$$

for any fixed point  $\mathbf{x}_0 \in \bar{\Omega}$ , where  $D$  is the diffusion coefficient, and  $\Delta$  is the Laplace operator [17]. This equation describes how the uncertainty on the location of the diffusing particle evolves with time from its initial deterministic location at a fixed starting point  $\mathbf{x}_0$ :

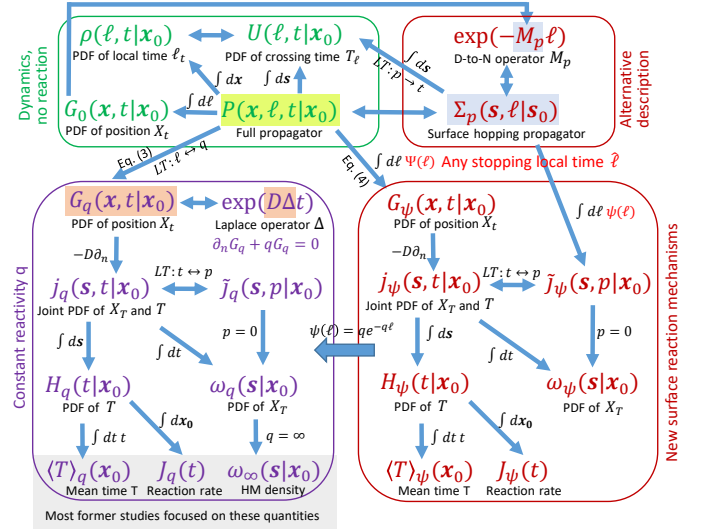


FIG. S2: Schematic view of interrelations between different functions describing diffusion and reactions. Top left frame includes the functions that characterize diffusion alone, without any reaction (reflecting boundary): the full propagator  $P(\mathbf{x}, \ell, t|\mathbf{x}_0)$ , the marginal propagator  $G_0(\mathbf{x}, t|\mathbf{x}_0)$  for zero reactivity, the probability density function (PDF)  $\rho(\ell, t|\mathbf{x}_0)$  of the boundary local time  $\ell_t$ , and the PDF  $U(\ell, t|\mathbf{x}_0)$  of the first-crossing time  $T_\ell$  of a level  $\ell$  by  $\ell_t$ . Top right frame illustrates our alternative description based on the surface hopping propagator  $\Sigma_p(\mathbf{s}, \ell|\mathbf{s}_0)$  and the associated Dirichlet-to-Neumann (D-to-N) operator  $\mathcal{M}_p$ , from which all other quantities can be derived (see arrows). Bottom left frame englobes the functions within the conventional description of partially reactive boundary by the Laplace operator  $\Delta$ , in which constant reactivity  $\kappa$  is implemented *implicitly* via Robin boundary condition with parameter  $q = \kappa/D$ : the conventional propagator  $G_q(\mathbf{x}, t|\mathbf{x}_0)$ , the probability flux density  $j_q(\mathbf{s}, t|\mathbf{x}_0)$  and its Laplace transform  $\tilde{j}_q(\mathbf{s}, p|\mathbf{x}_0)$ , the PDF  $H_q(t|\mathbf{x}_0)$  of the reaction time  $\mathcal{T}$  and the related survival probability, the PDF  $\omega_q(\mathbf{s}|\mathbf{x}_0)$  of the reaction location  $\mathbf{X}_\mathcal{T}$  on the boundary, the mean reaction time  $\langle \mathcal{T} \rangle_q(\mathbf{x}_0)$ , the reaction rate  $J_q(t)$ , and the harmonic measure (HM) density  $\omega_\infty(\mathbf{s}|\mathbf{x}_0)$ . Bottom right frame presents all the above quantities generalized to a variety of surface reaction mechanisms determined *explicitly* by the stopping local time  $\hat{\ell}$  with a given PDF  $\psi(\ell)$ . Note that the Laplace transform (LT) with respect to time  $t$  allows one to incorporate bulk reactivity  $p$  and thus to consider mortal walkers. Detailed relations between quantities are provided in Sec. SM.II and SM.IV.

$G_q(\mathbf{x}, t = 0|\mathbf{x}_0) = \delta(\mathbf{x} - \mathbf{x}_0)$ , where  $\delta(\mathbf{x})$  is the Dirac distribution. This equation is completed by the Robin boundary condition:

$$-\left(\partial_n G_q(\mathbf{x}, t|\mathbf{x}_0)\right)\Big|_{\mathbf{x}=\mathbf{s}} = q G_q(\mathbf{s}, t|\mathbf{x}_0) \quad (\mathbf{s} \in \partial\Omega), \quad (\text{S11})$$

where  $\partial_n$  is the normal derivative directed outward the domain  $\Omega$ , and  $q = \kappa/D$ . For unbounded domains, a regularity condition is also imposed at infinity:  $G_q(\mathbf{x}, t|\mathbf{x}_0) \rightarrow 0$  as  $|\mathbf{x}| \rightarrow \infty$ .

In [32, 40], several constructions of partially re-

flected Brownian motion, associated with the propagator  $G_q(\mathbf{x}, t|\mathbf{x}_0)$ , were discussed (see also [56, 57] for mathematical details and references). In particular, one can start from reflected Brownian motion  $\mathbf{X}_t$  in  $\Omega$  with *reflecting* boundary  $\partial\Omega$ , obtained as the solution of the Skorokhod equation (S6), and stop it at a random reaction time

$$\mathcal{T} := \inf\{t > 0 : \ell_t > \hat{\ell}\}, \quad (\text{S12})$$

when the boundary local time  $\ell_t$  exceeds an independent random variable  $\hat{\ell}$  with the exponential distribution:  $\mathbb{P}\{\hat{\ell} > \ell\} = e^{-q\ell}$ . In fact, as discussed in Sec. SM.I, the boundary local time  $\ell_t$  is related via Eq. (S9) to the number  $\mathcal{N}_t^a$  of encounters with a thin boundary layer of width  $a$ . At each encounter with the partially reactive boundary, the particle either reacts with the probability  $\Pi = 1/(1 + D/(\kappa a)) \simeq aq \ll 1$  (that follows from a discretization of Robin boundary condition (S11) at small scale  $a$ , see [31, 58]), or resumes its bulk diffusion with the probability  $1 - \Pi$ . If all reaction attempts are independent from each other, the number  $\hat{n}$  of failed attempts until the successful reaction follows the geometric law,  $\mathbb{P}\{\hat{n} > n\} = (1 - \Pi)^n \approx \exp(-qna)$ . The rescaled number of failed reaction attempts,  $\hat{\ell} = a\hat{n}$ , obeys thus the exponential law:  $\mathbb{P}\{\hat{\ell} > \ell\} = e^{-q\ell}$ , with  $\ell = an$ . As  $\hat{\ell} = \ell_{\mathcal{T}}$  by construction, the reaction time  $\mathcal{T}$  is defined by Eq. (S12), see [32, 40, 41] for details. After this reminder of the probabilistic construction of the reaction time  $\mathcal{T}$ , we are going to establish the fundamental representation (S14) for the conventional propagator, which to our knowledge is new.

The conventional propagator is by definition the probability density of the position  $\mathbf{X}_t$  of the *survived* particle at time  $t$ , i.e., of the particle that has not reacted up to time  $t$ :

$$G_q(\mathbf{x}, t|\mathbf{x}_0)d\mathbf{x} := \mathbb{P}_{\mathbf{x}_0}\{\mathbf{X}_t \in (\mathbf{x}, \mathbf{x} + d\mathbf{x}), t < \mathcal{T}\}. \quad (\text{S13})$$

As the boundary local time  $\ell_t$  is a nondecreasing process, the condition  $t < \mathcal{T}$  is equivalent to  $\ell_t < \hat{\ell}$  according to Eq. (S12). In other words, one has

$$\begin{aligned} G_q(\mathbf{x}, t|\mathbf{x}_0)d\mathbf{x} &= \mathbb{P}_{\mathbf{x}_0}\{\mathbf{X}_t \in (\mathbf{x}, \mathbf{x} + d\mathbf{x}), \ell_t < \hat{\ell}\} \\ &= \int_0^{\infty} d\ell \underbrace{q e^{-q\ell}}_{\text{pdf of } \hat{\ell}} \mathbb{P}_{\mathbf{x}_0}\{\mathbf{X}_t \in (\mathbf{x}, \mathbf{x} + d\mathbf{x}), \ell_t < \ell\} \\ &= \int_0^{\infty} d\ell q e^{-q\ell} \int_0^{\ell} d\ell' P(\mathbf{x}, \ell', t|\mathbf{x}_0)d\mathbf{x} \\ &= d\mathbf{x} \int_0^{\infty} d\ell e^{-q\ell} P(\mathbf{x}, \ell, t|\mathbf{x}_0), \end{aligned}$$

i.e.,

$$G_q(\mathbf{x}, t|\mathbf{x}_0) = \int_0^{\infty} d\ell e^{-q\ell} P(\mathbf{x}, \ell, t|\mathbf{x}_0). \quad (\text{S14})$$

Here we introduced the full propagator  $P(\mathbf{x}, \ell, t|\mathbf{x}_0)$  of reflected Brownian motion (without surface reaction), i.e., the joint probability density of the position  $\mathbf{X}_t$  and the boundary local time  $\ell_t$ . One sees that the exponential law of the stopping local time  $\hat{\ell}$  allowed us to represent the conventional propagator as the Laplace transform of the full propagator with respect to the local time  $\ell$ .

To proceed, we recall a useful representation of the conventional propagator from [27]:

$$\begin{aligned} G_q(\mathbf{x}, t|\mathbf{x}_0) &= G_{\infty}(\mathbf{x}, t|\mathbf{x}_0) + \int_{\partial\Omega} ds_1 \int_{\partial\Omega} ds_2 \int_0^t dt_1 \int_{t_1}^t dt_2 \\ &\times j_{\infty}(\mathbf{s}_2, t - t_2|\mathbf{x}) G_q(\mathbf{s}_2, t_2 - t_1|\mathbf{s}_1) j_{\infty}(\mathbf{s}_1, t_1|\mathbf{x}_0), \end{aligned} \quad (\text{S15})$$

where<sup>1</sup>

$$j_{\infty}(\mathbf{s}, t|\mathbf{x}_0) := - (D\partial_n G_{\infty}(\mathbf{x}, t|\mathbf{x}_0))|_{\mathbf{x}=\mathbf{s}} \quad (\text{S16})$$

is the probability flux density on a perfectly reactive boundary ( $q = \infty$ ), i.e., with  $G_{\infty}(\mathbf{x}, t|\mathbf{x}_0)$  satisfying Dirichlet boundary condition:  $G_{\infty}(\mathbf{x}, t|\mathbf{x}_0)|_{\mathbf{x} \in \partial\Omega} = 0$ . The representation (S15) has a straightforward probabilistic interpretation. The first term describes the contribution of direct trajectories from  $\mathbf{x}_0$  to  $\mathbf{x}$ , which do not hit the boundary over time from 0 to  $t$ . In turn, the second term provides the contribution for indirect trajectories: the particle first arrives at a boundary point  $\mathbf{s}_1$  at time  $t_1$  (factor  $j_{\infty}(\mathbf{s}_1, t_1|\mathbf{x}_0)$ ), then executes partially reflected Brownian motion until time  $t_2$  (factor  $G_q(\mathbf{s}_2, t_2 - t_1|\mathbf{s}_1)$ ), at which the particle leaves the boundary from a point  $\mathbf{s}_2$  and goes directly to the bulk point  $\mathbf{x}$  (factor  $j_{\infty}(\mathbf{s}_2, t - t_2|\mathbf{x})$ ). Expectedly, one integrates over intermediate boundary points  $\mathbf{s}_1$  and  $\mathbf{s}_2$  and times  $t_1$  and  $t_2$ .

The inverse Laplace transform of Eq. (S15) with respect to  $q$  yields, due to Eq. (S14), a similar representation for the full propagator:

$$\begin{aligned} P(\mathbf{x}, \ell, t|\mathbf{x}_0) &= G_{\infty}(\mathbf{x}, t|\mathbf{x}_0)\delta(\ell) + \int_{\partial\Omega} ds_1 \int_{\partial\Omega} ds_2 \int_0^t dt_1 \int_{t_1}^t dt_2 \\ &\times j_{\infty}(\mathbf{s}_2, t - t_2|\mathbf{x}) P(\mathbf{s}_2, \ell, t_2 - t_1|\mathbf{s}_1) j_{\infty}(\mathbf{s}_1, t_1|\mathbf{x}_0). \end{aligned} \quad (\text{S17})$$

The probabilistic interpretation is again straightforward. For a direct trajectory from  $\mathbf{x}_0$  to  $\mathbf{x}$ , which does not hit the boundary, the boundary local time remains unchanged (the first term). In turn, the increase of the boundary local time from 0 to  $\ell$  can only be achieved through indirect trajectories that hit the boundary (the

<sup>1</sup> We outline a confusing difference in notations between [27] and the present paper: in [27], the subscript 0 referred to the perfectly reactive boundary that we denote here by the subscript  $\infty$ .

second term). In this way, the full propagator for arbitrary points  $\mathbf{x}$  and  $\mathbf{x}_0$  is expressed in terms of the full propagator for boundary points  $\mathbf{s}_1$  and  $\mathbf{s}_2$ .

The Laplace transform of Eq. (S17) with respect to  $t$  reduces time convolutions:

$$\begin{aligned} \tilde{P}(\mathbf{x}, \ell, p | \mathbf{x}_0) &= \tilde{G}_\infty(\mathbf{x}, p | \mathbf{x}_0) \delta(\ell) \\ &+ \int_{\partial\Omega} d\mathbf{s}_1 \int_{\partial\Omega} d\mathbf{s}_2 \tilde{j}_\infty(\mathbf{s}_2, p | \mathbf{x}) \tilde{P}(\mathbf{s}_2, \ell, p | \mathbf{s}_1) \tilde{j}_\infty(\mathbf{s}_1, p | \mathbf{x}_0), \end{aligned} \quad (\text{S18})$$

where tilde denotes Laplace-transformed quantities (with respect to  $t$ ), e.g.,

$$\tilde{P}(\mathbf{x}, \ell, p | \mathbf{x}_0) := \int_0^\infty dt e^{-pt} P(\mathbf{x}, \ell, t | \mathbf{x}_0). \quad (\text{S19})$$

In particular, for a boundary point  $\mathbf{x} = \mathbf{s} \in \partial\Omega$ , the first term vanishes, whereas  $\tilde{j}_\infty(\mathbf{s}_2, p | \mathbf{s}) = \delta(\mathbf{s}_2 - \mathbf{s})$ , so that

$$\tilde{P}(\mathbf{s}, \ell, p | \mathbf{x}_0) = \int_{\partial\Omega} d\mathbf{s}_1 \tilde{P}(\mathbf{s}, \ell, p | \mathbf{s}_1) \tilde{j}_\infty(\mathbf{s}_1, p | \mathbf{x}_0). \quad (\text{S20})$$

## B. Surface hopping propagator

To express  $\tilde{P}(\mathbf{s}_2, \ell, p | \mathbf{s}_1)$ , we now introduce the surface hopping propagator  $\Sigma_p(\mathbf{s}, \ell | \mathbf{s}_0)$ . For this purpose, we compute the marginal probability density of the reaction position  $\mathbf{X}_\mathcal{T}$  by two alternative ways.

On one hand, we define the surface hopping propagator  $\Sigma_p(\mathbf{s}, \ell | \mathbf{s}_0)$  as the probability density of finding a particle, started from a boundary point  $\mathbf{s}_0$  and survived bulk reaction with a rate  $p$ , in a boundary point  $\mathbf{s}$  at the local time  $\ell$ . Since the surface reaction occurs at a random, exponentially distributed stopping local time  $\hat{\ell}$ , which is independent of the particle's motion, the probability density of the reaction position  $\mathbf{X}_\mathcal{T}$  can be obtained by averaging  $\Sigma_p(\mathbf{s}, \hat{\ell} | \mathbf{s}_0)$  with the exponential density  $qe^{-q\ell}$  for  $\hat{\ell}$ :

$$\int_0^\infty d\ell qe^{-q\ell} \Sigma_p(\mathbf{s}, \ell | \mathbf{s}_0). \quad (\text{S21})$$

On the other hand, the conventional propagator determines the probability flux density at a boundary point  $\mathbf{s} \in \partial\Omega$ :

$$j_q(\mathbf{s}, t | \mathbf{x}_0) := -D (\partial_n G_q(\mathbf{x}, t | \mathbf{x}_0)) \Big|_{\mathbf{x}=\mathbf{s}}, \quad (\text{S22})$$

i.e., the joint probability density of the stopping position  $\mathbf{X}_\mathcal{T}$  on the boundary and of the stopping time  $\mathcal{T}$ :

$$j_q(\mathbf{s}, t | \mathbf{x}_0) d\mathbf{s} dt = \mathbb{P}_{\mathbf{x}_0} \{ \mathbf{X}_\mathcal{T} \in (\mathbf{s}, \mathbf{s} + d\mathbf{s}), \mathcal{T} \in (t, t + dt) \}. \quad (\text{S23})$$

Note that Robin boundary condition (S11) yields an equivalent relation

$$j_q(\mathbf{s}, t | \mathbf{x}_0) = qDG_q(\mathbf{s}, t | \mathbf{x}_0). \quad (\text{S24})$$

For a particle with a finite random lifetime  $\hat{t}$  due to bulk reaction, one needs to include the additional condition that the particle has reacted on the surface during its lifetime (i.e., before its death):  $\mathcal{T} < \hat{t}$ . Since  $\hat{t}$  is independent from both  $\mathbf{X}_t$  and  $\mathcal{T}$ , one has

$$\begin{aligned} \mathbb{P}_{\mathbf{x}_0} \{ \mathbf{X}_\mathcal{T} \in (\mathbf{s}, \mathbf{s} + d\mathbf{s}), \mathcal{T} \in (t, t + dt), \mathcal{T} < \hat{t} \} \\ = \mathbb{P} \{ \hat{t} > t \} j_q(\mathbf{s}, t | \mathbf{x}_0) dt d\mathbf{s}, \end{aligned}$$

where  $\mathbb{P} \{ \hat{t} > t \} = e^{-pt}$  for the considered Poissonian-type bulk reaction with the rate  $p$ . The integral of this probability density over  $t$  yields the marginal probability density of the reaction position  $\mathbf{X}_\mathcal{T}$  (for the particle that survived bulk reaction), which turns out to coincide with the Laplace transform of  $j_q(\mathbf{s}, t | \mathbf{x}_0)$ :

$$\tilde{j}_q(\mathbf{s}, p | \mathbf{x}_0) := \int_0^\infty dt e^{-pt} j_q(\mathbf{s}, t | \mathbf{x}_0). \quad (\text{S25})$$

When the starting point  $\mathbf{x}_0$  lies on the boundary,  $\mathbf{x}_0 = \mathbf{s}_0 \in \partial\Omega$ ,  $\tilde{j}_q(\mathbf{s}, p | \mathbf{s}_0)$  is identical, by construction, to the probability density of  $\mathbf{X}_\mathcal{T}$  given by Eq. (S21):

$$\tilde{j}_q(\mathbf{s}, p | \mathbf{s}_0) = \int_0^\infty d\ell qe^{-q\ell} \Sigma_p(\mathbf{s}, \ell | \mathbf{s}_0). \quad (\text{S26})$$

Expressing the left-hand side with the aid of Eq. (S24), we can re-write this relation more explicitly in terms of two Laplace transforms:

$$D \int_0^\infty dt e^{-pt} G_q(\mathbf{s}, t | \mathbf{s}_0) = \int_0^\infty d\ell e^{-q\ell} \Sigma_p(\mathbf{s}, \ell | \mathbf{s}_0). \quad (\text{S27})$$

This fundamental identity relates the conventional propagator  $G_q(\mathbf{s}, t | \mathbf{s}_0)$  to the surface hopping propagator  $\Sigma_p(\mathbf{s}, \ell | \mathbf{s}_0)$ . This relation highlights the duality between bulk and surface reaction mechanisms which involve time  $t$  and local time  $\ell$  via respective Laplace transforms. Even so Eq. (S27) determines  $G_q(\mathbf{s}, t | \mathbf{s}_0)$  only at boundary points  $\mathbf{s}$  and  $\mathbf{s}_0$ , the propagator  $G_q(\mathbf{x}, t | \mathbf{x}_0)$  can then be recovered from Eq. (S15) for all bulk points  $\mathbf{x}$  and  $\mathbf{x}_0$ .

Comparing the identity (S27) to Eq. (S14), evaluated at  $\mathbf{x} = \mathbf{s}$  and  $\mathbf{x}_0 = \mathbf{s}_0$ , we also conclude that

$$\Sigma_p(\mathbf{s}, \ell | \mathbf{s}_0) = D \int_0^\infty dt e^{-pt} P(\mathbf{s}, \ell, t | \mathbf{s}_0). \quad (\text{S28})$$

Bearing in mind this relation, one finally realizes that the identity (S27) reflects a very simple statement: if there are both bulk and surface reaction mechanisms, the order of implementation of these mechanisms does not matter. In fact, the conventional approach consists in incorporating first the surface reactivity via the Robin boundary condition to get  $G_q(\mathbf{s}, t | \mathbf{s}_0)$  and then averaging it with the

survival probability  $\mathbb{P}\{\hat{t} > t\} = e^{-pt}$  to include bulk reaction (the left-hand side of Eq. (S27)). In turn, the alternative description proposed here consists in implementing first the bulk reactivity via Eq. (S28) and then averaging the surface hopping propagator  $\Sigma_p(\mathbf{s}, \ell | \mathbf{s}_0)$  with the probability density  $qe^{-q\ell}$  of the stopping local time  $\hat{t}$  to include surface reaction (the right-hand side of Eq. (S27)). Note also that the inverse Laplace transform of Eq. (S28) with respect to  $p$  reads

$$P(\mathbf{s}, \ell, t | \mathbf{s}_0) = \frac{1}{D} \mathcal{L}_t^{-1} \{ \Sigma_p(\mathbf{s}, \ell | \mathbf{s}_0) \}. \quad (\text{S29})$$

Substitution of Eq. (S28) into Eq. (S18) yields

$$\begin{aligned} \tilde{P}(\mathbf{x}, \ell, p | \mathbf{x}_0) &= \tilde{G}_\infty(\mathbf{x}, p | \mathbf{x}_0) \delta(\ell) \\ &+ \int_{\partial\Omega} ds_1 \int_{\partial\Omega} ds_2 \tilde{j}_\infty(\mathbf{s}_2, p | \mathbf{x}) \frac{\Sigma_p(\mathbf{s}_2, \ell | \mathbf{s}_1)}{D} \tilde{j}_\infty(\mathbf{s}_1, p | \mathbf{x}_0), \end{aligned} \quad (\text{S30})$$

i.e., the surface hopping propagator, together with  $\tilde{G}_\infty(\mathbf{x}, p | \mathbf{x}_0)$ , determines the full propagator  $P(\mathbf{x}, \ell, t | \mathbf{x}_0)$  in the Laplace domain. This relation is the basis for computing the full propagator.

### C. Dirichlet-to-Neumann operator

The last step consists in deriving the spectral decomposition of the surface hopping propagator on the basis of the Dirichlet-to-Neumann operator  $\mathcal{M}_p$ . For a given function  $f$  on the boundary  $\partial\Omega$ , the operator  $\mathcal{M}_p$  associates another function  $g = \mathcal{M}_p f = (\partial_n w)|_{\partial\Omega}$ , where  $w$  is the solution of the Dirichlet boundary value problem for the modified Helmholtz equation:

$$(p - D\Delta)w = 0 \quad (\mathbf{x} \in \Omega), \quad w|_{\partial\Omega} = f \quad (\text{S31})$$

(with the regularity condition  $w(\mathbf{x}) \rightarrow 0$  as  $|\mathbf{x}| \rightarrow \infty$  if  $\Omega$  is not bounded). The Dirichlet-to-Neumann operator  $\mathcal{M}_p$  is a self-adjoint pseudo-differential operator (see [59–63]). On one hand, the action of the Dirichlet-to-Neumann operator on a function  $f(\mathbf{s})$  on the boundary can be expressed by solving the boundary value problem (S31) in a standard way with the help of the Laplace-transformed propagator  $\tilde{G}_\infty(\mathbf{x}, p | \mathbf{x}_0)$  with Dirichlet boundary condition ( $q = \infty$ ):

$$\begin{aligned} [\mathcal{M}_p f](\mathbf{s}_0) & \\ &= \left( \partial_{n_0} \int_{\partial\Omega} ds \underbrace{(-D\partial_n \tilde{G}_\infty(\mathbf{x}, p | \mathbf{x}_0))}_{=\tilde{j}_\infty(\mathbf{s}, p | \mathbf{x}_0)} \Big|_{\mathbf{x}=\mathbf{s}} f(\mathbf{s}) \right)_{\mathbf{x}_0=\mathbf{s}_0}. \end{aligned} \quad (\text{S32})$$

On the other hand, the inverse of the Dirichlet-to-Neumann operator  $\mathcal{M}_p$  with  $p > 0$  can be expressed in terms of the Laplace-transformed propagator  $\tilde{G}_0(\mathbf{x}, p | \mathbf{x}_0)$  with Neumann boundary condition ( $q = 0$ ) [27]:

$$D\tilde{G}_0(\mathbf{s}, p | \mathbf{s}_0) = \mathcal{M}_p^{-1} \delta(\mathbf{s} - \mathbf{s}_0) \quad (\mathbf{s}, \mathbf{s}_0 \in \partial\Omega). \quad (\text{S33})$$

More generally,  $\tilde{G}_q(\mathbf{s}, p | \mathbf{s}_0)$  was shown to be related to the resolvent of the Dirichlet-to-Neumann operator [27]:

$$D\tilde{G}_q(\mathbf{s}, p | \mathbf{s}_0) = (qI + \mathcal{M}_p)^{-1} \delta(\mathbf{s} - \mathbf{s}_0), \quad (\text{S34})$$

where  $I$  is the identity operator. Substituting this expression into Eq. (S27) and performing the inverse Laplace transform with respect to  $q$ , we show that

$$\Sigma_p(\mathbf{s}, \ell | \mathbf{s}_0) = \exp(-\mathcal{M}_p \ell) \delta(\mathbf{s} - \mathbf{s}_0), \quad (\text{S35})$$

i.e., the surface hopping propagator is the kernel of the semigroup  $\exp(-\mathcal{M}_p \ell)$  associated with the Dirichlet-to-Neumann operator  $\mathcal{M}_p$ . Taking the derivative with respect to  $\ell$ , one immediately gets

$$\partial_\ell \Sigma_p(\mathbf{s}, \ell | \mathbf{s}_0) = -\mathcal{M}_p \Sigma_p(\mathbf{s}, \ell | \mathbf{s}_0), \quad (\text{S36})$$

subject to the initial condition with Dirac distribution:

$$\Sigma_p(\mathbf{s}, \ell = 0 | \mathbf{s}_0) = \delta(\mathbf{s} - \mathbf{s}_0). \quad (\text{S37})$$

This is a sort of diffusion equation characterizing surface exploration by bulk-mediated diffusion hops on the boundary, whose “number” is quantified by the boundary local time  $\ell$ , in analogy with bulk jumps of a random walk quantified by the physical time  $t$ .

When the boundary  $\partial\Omega$  is bounded, the Dirichlet-to-Neumann operator  $\mathcal{M}_p$  has a discrete spectrum, i.e., a countable set of eigenvalues  $\mu_n^{(p)}$  and eigenfunctions  $v_n^{(p)}(\mathbf{s})$  satisfying

$$\mathcal{M}_p v_n^{(p)}(\mathbf{s}) = \mu_n^{(p)} v_n^{(p)}(\mathbf{s}). \quad (\text{S38})$$

The eigenvalues are nonnegative, whereas the eigenfunctions form an orthonormal complete basis in the space  $L_2(\partial\Omega)$  of square-integrable functions on the boundary  $\partial\Omega$ . We emphasize that this property holds irrespectively of whether the domain  $\Omega$  is bounded or not. In the bounded case, Eqs. (S34, S35) imply the spectral decompositions:

$$D\tilde{G}_q(\mathbf{s}, p | \mathbf{s}_0) = \sum_n [v_n^{(p)}(\mathbf{s}_0)]^* v_n^{(p)}(\mathbf{s}) \frac{1}{q + \mu_n^{(p)}} \quad (\text{S39})$$

and

$$\Sigma_p(\mathbf{s}, \ell | \mathbf{s}_0) = \sum_n [v_n^{(p)}(\mathbf{s}_0)]^* v_n^{(p)}(\mathbf{s}) \exp(-\mu_n^{(p)} \ell), \quad (\text{S40})$$

where asterisk denotes the complex conjugate. The completeness of the eigenfunctions  $v_n^{(p)}(\mathbf{s})$  ensures the correct initial condition (S37). Substituting Eq. (S40) into Eq. (S30), we derive the spectral expansion of the Laplace-transformed full propagator:

$$\begin{aligned} \tilde{P}(\mathbf{x}, \ell, p | \mathbf{x}_0) &= \tilde{G}_\infty(\mathbf{x}, p | \mathbf{x}_0) \delta(\ell) \\ &+ \frac{1}{D} \sum_n [V_n^{(p)}(\mathbf{x}_0)]^* V_n^{(p)}(\mathbf{x}) \exp(-\mu_n^{(p)} \ell), \end{aligned} \quad (\text{S41})$$

where

$$V_n^{(p)}(\mathbf{x}_0) := \int_{\partial\Omega} d\mathbf{s}_0 v_n^{(p)}(\mathbf{s}_0) \tilde{j}_\infty(\mathbf{s}_0, p|\mathbf{x}_0) \quad (\text{S42})$$

is the projection of  $\tilde{j}_\infty(\mathbf{s}_0, p|\mathbf{x}_0)$  onto the eigenfunction  $v_n^{(p)}$  of the Dirichlet-to-Neumann operator. By construction, each function  $V_n^{(p)}(\mathbf{x})$  satisfies the modified Helmholtz equation (S31) with Dirichlet boundary condition,  $(V_n^{(p)})|_{\partial\Omega} = v_n^{(p)}$ , i.e., they naturally appear in the definition of the Dirichlet-to-Neumann operator  $\mathcal{M}_p$ ; in particular,  $(\partial_n V_n^{(p)})|_{\partial\Omega} = \mu_n^{(p)} v_n^{(p)}$ .

The profound relation (S27) between the conventional propagator and the surface hopping propagator allows one to derive new spectral decompositions for many quantities characterizing diffusion-influenced reactions. For instance, Eq. (S26), written more generally for a bulk starting point  $\mathbf{x}_0$  (instead of  $\mathbf{s}_0$ ), yields

$$\tilde{j}_q(\mathbf{s}, p|\mathbf{x}_0) = \sum_n [V_n^{(p)}(\mathbf{x}_0)]^* v_n^{(p)}(\mathbf{s}) \frac{q}{q + \mu_n^{(p)}}, \quad (\text{S43})$$

which was earlier reported in [27]. Other spectral expansions will be provided in Sec. SM.IV.

#### D. Boundary value problem for the full propagator

The full propagator  $P(\mathbf{x}, \ell, t|\mathbf{x}_0)$  is determined in the Laplace domain by Eq. (S30), which depends on the surface hopping propagator and thus can be computed from the spectral properties of the Dirichlet-to-Neumann operator. Nevertheless, it is instructive to formulate the boundary value problem for the full propagator.

As the first term of the Skorokhod equation (S6) affects reflected Brownian motion only on the boundary, the full propagator is expected to obey the ordinary diffusion equation in the bulk

$$\partial_t P(\mathbf{x}, \ell, t|\mathbf{x}_0) = D\Delta P(\mathbf{x}, \ell, t|\mathbf{x}_0), \quad (\text{S44})$$

subject to the initial condition

$$P(\mathbf{x}, \ell, t = 0|\mathbf{x}_0) = \delta(\mathbf{x} - \mathbf{x}_0)\delta(\ell). \quad (\text{S45})$$

This property can be checked by applying the operator  $(p - D\Delta)$  to Eq. (S18) that yields

$$(p - D\Delta)\tilde{P}(\mathbf{x}, \ell, p|\mathbf{x}_0) = \delta(\mathbf{x} - \mathbf{x}_0)\delta(\ell). \quad (\text{S46})$$

In fact, the second term of Eq. (S18) vanishes since  $(p - D\Delta)\tilde{j}_\infty(\mathbf{s}_2, p|\mathbf{x}) = 0$  for any bulk point  $\mathbf{x} \in \Omega$ , and we used that  $(p - D\Delta)\tilde{G}_\infty(\mathbf{x}, p|\mathbf{x}_0) = \delta(\mathbf{x} - \mathbf{x}_0)$ . The inverse Laplace transform of Eq. (S46) implies Eqs. (S44, S45).

In turn, the boundary local time increases at each encounter with the boundary, so that its effect should be taken into account via an appropriate boundary condition. As changes of the full propagator with respect to

$\ell$  are driven by arrivals of the particle onto the boundary, the derivative of  $P(\mathbf{x}, \ell, t|\mathbf{x}_0)$  with respect to  $\ell$  is expected to be related to the normal derivative of the full propagator on the boundary. To establish this relation, we first evaluate the normal derivative of the Laplace-transformed full propagator in Eq. (S30):

$$\begin{aligned} -D(\partial_n \tilde{P}(\mathbf{x}, \ell, p|\mathbf{x}_0))\Big|_{\mathbf{x}=\mathbf{s}} &= \tilde{j}_\infty(\mathbf{s}, p|\mathbf{x}_0) \delta(\ell) \quad (\text{S47}) \\ &- \int_{\partial\Omega} d\mathbf{s}_1 \tilde{j}_\infty(\mathbf{s}_1, p|\mathbf{x}_0) \\ &\times \left( \partial_n \int_{\partial\Omega} d\mathbf{s}_2 \tilde{j}_\infty(\mathbf{s}_2, p|\mathbf{x}) \Sigma_p(\mathbf{s}_2, \ell|\mathbf{s}_1) \right)\Big|_{\mathbf{x}=\mathbf{s}}. \end{aligned}$$

According to Eq. (S32), the factor in the last line can be interpreted as the action of the Dirichlet-to-Neumann operator  $\mathcal{M}_p$  on  $\Sigma_p(\cdot, \ell|\mathbf{s}_1)$ ; in turn, Eqs. (S20, S36) imply

$$\begin{aligned} -D(\partial_n \tilde{P}(\mathbf{x}, \ell, p|\mathbf{x}_0))\Big|_{\mathbf{x}=\mathbf{s}} &= \tilde{j}_\infty(\mathbf{s}, p|\mathbf{x}_0) \delta(\ell) \\ &+ D\partial_\ell \tilde{P}(\mathbf{s}, \ell, p|\mathbf{x}_0). \quad (\text{S48}) \end{aligned}$$

The inverse Laplace transform of this relation with respect to  $p$  yields the desired boundary condition for the full propagator:

$$\begin{aligned} -D(\partial_n P(\mathbf{x}, \ell, t|\mathbf{x}_0))\Big|_{\mathbf{x}=\mathbf{s}} &= j_\infty(\mathbf{s}, t|\mathbf{x}_0) \delta(\ell) \\ &+ D\partial_\ell P(\mathbf{s}, \ell, t|\mathbf{x}_0). \quad (\text{S49}) \end{aligned}$$

In addition, one has

$$P(\mathbf{s}, \ell = 0, t|\mathbf{x}_0) = \frac{1}{D} j_\infty(\mathbf{s}, t|\mathbf{x}_0) \quad (\mathbf{s} \in \partial\Omega), \quad (\text{S50})$$

which follows from the inverse Laplace transform of Eq. (S41) evaluated at  $\mathbf{x} = \mathbf{s} \in \partial\Omega$  and  $\ell = 0$  and using Eq. (S37).

To complete the formulation, one also needs to impose the regularity condition

$$\lim_{\ell \rightarrow \infty} P(\mathbf{x}, \ell, t|\mathbf{x}_0) = 0, \quad (\text{S51})$$

ensuring that the boundary local time cannot be infinite within a finite time  $t$ . For unbounded domains, a similar regularity condition on  $\mathbf{x}$  is imposed:

$$\lim_{|\mathbf{x}| \rightarrow \infty} P(\mathbf{x}, \ell, t|\mathbf{x}_0) = 0. \quad (\text{S52})$$

The boundary value problem (S44, S45, S49, S50, S51, S52) determines the full propagator  $P(\mathbf{x}, \ell, t|\mathbf{x}_0)$ .

Multiplying the boundary condition (S49) by  $e^{-q\ell}$ , integrating over  $\ell$  from 0 to  $\infty$ , and performing integration by parts in the last term, one retrieves Robin boundary condition (S11) for the conventional propagator  $G_q(\mathbf{x}, t|\mathbf{x}_0)$ , where we used Eq. (S50).

### E. Distribution of the boundary local time

By definition, the integral of the full propagator  $P(\mathbf{x}, \ell, t|\mathbf{x}_0)$  over the arrival point  $\mathbf{x}$  gives the marginal probability density of the boundary local time  $\ell_t$ :

$$\rho(\ell, t|\mathbf{x}_0) := \int_{\Omega} d\mathbf{x} P(\mathbf{x}, \ell, t|\mathbf{x}_0). \quad (\text{S53})$$

The properties of the boundary local time were discussed in Sec. [SM.I](#).

The probability density in Eq. [\(S53\)](#) can be expressed in terms of the surface hopping propagator. For this purpose, it is convenient to work in the Laplace domain, in which the integral of Eq. [\(S30\)](#) over  $\mathbf{x}$  yields

$$\begin{aligned} \tilde{\rho}(\ell, p|\mathbf{x}_0) &= \tilde{S}_{\infty}(p|\mathbf{x}_0)\delta(\ell) \\ &+ \int_{\partial\Omega} ds_1 \int_{\partial\Omega} ds_2 \frac{D}{p} [\mathcal{M}_p 1](s_2) \frac{\Sigma_p(s_2, \ell|\mathbf{s}_1)}{D} \tilde{j}_{\infty}(s_1, p|\mathbf{x}_0), \end{aligned} \quad (\text{S54})$$

where we used the identity

$$\int_{\Omega} d\mathbf{x} \tilde{j}_{\infty}(s_2, p|\mathbf{x}) = \frac{D}{p} [\mathcal{M}_p 1](s_2) \quad (\text{S55})$$

derived in [\[27\]](#), and

$$\tilde{S}_{\infty}(p|\mathbf{x}_0) := \int_{\Omega} d\mathbf{x} \tilde{G}_{\infty}(\mathbf{x}, p|\mathbf{x}_0) \quad (\text{S56})$$

is the Laplace-transformed survival probability for a perfectly reactive boundary. Writing the second integral in Eq. [\(S54\)](#) in the form of a scalar product, one has

$$\begin{aligned} (\Sigma_p(\cdot, \ell|\mathbf{s}_1) \cdot \mathcal{M}_p 1)_{L_2(\partial\Omega)} &= (\mathcal{M}_p \Sigma_p(\cdot, \ell|\mathbf{s}_1) \cdot 1)_{L_2(\partial\Omega)} \\ &= (-\partial_{\ell} \Sigma_p(\cdot, \ell|\mathbf{s}_1) \cdot 1)_{L_2(\partial\Omega)} = -\partial_{\ell} \int_{\partial\Omega} ds_2 \Sigma_p(s_2, \ell|\mathbf{s}_1), \end{aligned}$$

where we used Eq. [\(S36\)](#). The integral of  $\Sigma_p(s_2, \ell|\mathbf{s}_1)$  over  $s_2$  is the probability that the particle is survived the bulk reaction up to the local time  $\ell$ . In other words, this is the probability that the boundary local time  $\ell_t$ , stopped at  $t = \hat{t}$ , exceeds  $\ell$ :

$$\begin{aligned} \int_{\partial\Omega} ds_2 \Sigma_p(s_2, \ell|\mathbf{s}_1) &= \mathbb{P}_{\mathbf{s}_1} \{\ell_t > \ell\} \\ &= \int_0^{\infty} dt p e^{-pt} \mathbb{P}_{\mathbf{s}_1} \{\ell_t > \ell\}. \end{aligned} \quad (\text{S57})$$

We get thus

$$\begin{aligned} (\Sigma_p(\cdot, \ell|\mathbf{s}_1) \cdot \mathcal{M}_p 1)_{L_2(\partial\Omega)} &= -\partial_{\ell} \int_0^{\infty} dt p e^{-pt} \mathbb{P}_{\mathbf{s}_1} \{\ell_t > \ell\} \\ &= p \tilde{\rho}(\ell, p|\mathbf{s}_1), \end{aligned}$$

from which

$$\tilde{\rho}(\ell, p|\mathbf{s}_0) = -\partial_{\ell} \frac{1}{p} \int_{\partial\Omega} ds \Sigma_p(s, \ell|\mathbf{s}_0). \quad (\text{S58})$$

As a consequence, Eq. [\(S54\)](#) is reduced to

$$\tilde{\rho}(\ell, p|\mathbf{x}_0) = \tilde{S}_{\infty}(p|\mathbf{x}_0)\delta(\ell) + \int_{\partial\Omega} ds \tilde{\rho}(\ell, p|\mathbf{s}) \tilde{j}_{\infty}(s, p|\mathbf{x}_0), \quad (\text{S59})$$

which was reported in [\[41\]](#).

Moreover, the Laplace transform of Eq. [\(S53\)](#) with respect to  $\ell$ , together with Eq. [\(S14\)](#), yields

$$\mathbb{E}_{\mathbf{x}_0} \{e^{-q\ell_t}\} = \int_0^{\infty} d\ell e^{-q\ell} \rho(\ell, t|\mathbf{x}_0) = S_q(t|\mathbf{x}_0), \quad (\text{S60})$$

where

$$S_q(t|\mathbf{x}_0) := \int_{\Omega} d\mathbf{x} G_q(\mathbf{x}, t|\mathbf{x}_0) \quad (\text{S61})$$

is the survival probability for partially reactive boundary. This relation allows one to interpret the survival probability  $S_q(t|\mathbf{x}_0)$  as the moment-generating function of the boundary local time  $\ell_t$ . Similarly, Eq. [\(S14\)](#) provides an interpretation of the conventional propagator  $G_q(\mathbf{x}, t|\mathbf{x}_0)$  as the moment-generating function of the boundary local time  $\ell_t$  with the constraint on the position  $\mathbf{X}_t$ :

$$G_q(\mathbf{x}, t|\mathbf{x}_0) = \mathbb{E}_{\mathbf{x}_0} \{\exp(-q\ell_t) \delta(\mathbf{X}_t - \mathbf{x})\}. \quad (\text{S62})$$

To our knowledge, these representations were not reported earlier.

It is also instructive to reconsider the approximation  $\ell_t^a$  of the boundary local time  $\ell_t$  as the residence time in a thin boundary layer  $\partial\Omega_a$  of width  $a$ , rescaled by  $D/a$ , see Eq. [\(S3\)](#). We introduce its moment-generating function with the constraint on the position  $\mathbf{X}_t$ :

$$G_q^a(\mathbf{x}, t|\mathbf{x}_0) = \mathbb{E}_{\mathbf{x}_0} \{\exp(-q\ell_t^a) \delta(\mathbf{X}_t - \mathbf{x})\}. \quad (\text{S63})$$

According to the Feynman-Kac formula [\[34\]](#), this function satisfies the backward Fokker-Planck equation, which can be written in the forward form due to the time reversal symmetry:

$$\partial_t G_q^a(\mathbf{x}, t|\mathbf{x}_0) = \left( D\Delta - \frac{qD}{a} \mathbb{I}_{\partial\Omega_a}(\mathbf{x}) \right) G_q^a(\mathbf{x}, t|\mathbf{x}_0), \quad (\text{S64})$$

subject to the initial condition  $G_q^a(\mathbf{x}, t|\mathbf{x}_0) = \delta(\mathbf{x} - \mathbf{x}_0)$  and Neumann boundary condition  $(\partial_n G_q^a(\mathbf{x}, t|\mathbf{x}_0))|_{\mathbf{x} \in \partial\Omega} = 0$ . This equation can be interpreted as diffusion in  $\Omega$  with reflecting boundary subject to *bulk* reaction in the thin boundary layer  $\partial\Omega_a$  with the rate  $qD/a = \kappa/a$ . In the limit  $a \rightarrow 0$ ,  $\ell_t^a$  approaches  $\ell_t$  due to Eq. [\(S5\)](#) so that  $G_q^a(\mathbf{x}, t|\mathbf{x}_0)$

is expected to approach the conventional propagator  $G_q(\mathbf{x}, t|\mathbf{x}_0)$ . The equivalence of two descriptions was earlier discussed in [64]. It also resembles the basic idea of the diffuse layer approximation, in which a sharp boundary is replaced by a diffuse layer in order to represent boundary conditions by appropriate bulk terms [65, 66].

### F. Distribution of the first-crossing time

As surface reaction occurs at a random time  $\mathcal{T}$  when the boundary local time  $\ell_t$  exceeds the random stopping local time  $\hat{\ell}$ , it is natural to look at the distribution of the first-crossing time  $T_\ell$  of a fixed threshold  $\ell$ .

Let  $U(\ell, t|\mathbf{x}_0)$  denote the probability density of the first moment  $T_\ell$  when the boundary local time  $\ell_t$  exceeds  $\ell$ :

$$T_\ell := \inf\{t > 0 : \ell_t > \ell\}. \quad (\text{S65})$$

Since the boundary local time is a nondecreasing process, one has

$$\mathbb{P}_{\mathbf{x}_0}\{\ell_t > \ell\} = \mathbb{P}_{\mathbf{x}_0}\{t > T_\ell\}, \quad (\text{S66})$$

from which the probability density of  $T_\ell$  follows:

$$U(\ell, t|\mathbf{x}_0) = \partial_t \mathbb{P}_{\mathbf{x}_0}\{t > T_\ell\} = \partial_t \int_\ell^\infty d\ell' \rho(\ell', t|\mathbf{x}_0), \quad (\text{S67})$$

where  $\rho(\ell, t|\mathbf{x}_0)$  is the probability density of the boundary local time  $\ell_t$ . Applying the Laplace transform with respect to  $t$  and using Eqs. (S58, S59) for  $\tilde{\rho}(\ell, p|\mathbf{x}_0)$ , we get

$$\tilde{U}(\ell, p|\mathbf{x}_0) = p \int_\ell^\infty d\ell' \tilde{\rho}(\ell', p|\mathbf{x}_0) = \int_{\partial\Omega} ds D \tilde{P}(\mathbf{s}, \ell, p|\mathbf{x}_0). \quad (\text{S68})$$

The spectral expansion (S41) yields

$$\tilde{U}(\ell, p|\mathbf{x}_0) = \sum_n e^{-\mu_n^{(p)} \ell} [V_n^{(p)}(\mathbf{x}_0)]^* \int_{\partial\Omega} ds v_n^{(p)}(\mathbf{s}). \quad (\text{S69})$$

The inverse Laplace transform of Eq. (S68) with respect to  $p$  also gives

$$U(\ell, t|\mathbf{x}_0) = D \int_{\partial\Omega} ds P(\mathbf{s}, \ell, t|\mathbf{x}_0). \quad (\text{S70})$$

While the integral of the full propagator  $P(\mathbf{x}, \ell, t|\mathbf{x}_0)$  over bulk points  $\mathbf{x} \in \Omega$  in Eq. (S53) yields the marginal probability density  $\rho(\ell, t|\mathbf{x}_0)$  of the boundary local time, its integral over boundary points  $\mathbf{s} \in \partial\Omega$ , multiplied by  $D$ , determines the probability density  $U(\ell, t|\mathbf{x}_0)$  of the first-crossing time  $T_\ell$ .

The density  $U(\ell, t|\mathbf{x}_0)$  characterizes the dynamics of a diffusing particle near a fully reflecting boundary (without any reaction) and will thus play the central role

in the analysis of the reaction time (see Sec. SM.IV). For instance, as the first crossing of the level  $\ell = 0$  corresponds to the first arrival of the particle onto the boundary,  $U(0, t|\mathbf{x}_0)$  is the probability density of the first-passage time to the boundary. Most former studies of first-passage properties were limited to this quantity, which characterizes a perfectly reactive boundary.

### SM.III. ENCOUNTER-DEPENDENT REACTIVITY

In the conventional description, at each encounter with a partially reactive surface, the particle either reacted with a constant probability  $\Pi \approx a\kappa/D \ll 1$ , or resumed its bulk diffusion with probability  $1 - \Pi$ . We extend this description to account for variable, encounter-dependent reactivity that can model progressive passivation/activation or aging of the reactive surface after each reaction attempt. We consider now that, at  $n$ -th encounter with the boundary, the reaction probability is  $\Pi_n \approx a\kappa_n/D$ , with a given infinite sequence of reactivities  $\kappa_n$ . If reaction attempts are independent, then the probability of reaction exactly after  $n$  failed attempts is

$$\mathbb{P}\{\hat{n} = n\} = (1 - \Pi_0)(1 - \Pi_1) \dots (1 - \Pi_{n-1})\Pi_n, \quad (\text{S71})$$

(with  $n = 0, 1, 2, \dots$ ), whereas the probability of at least  $n$  failed attempts is

$$\mathbb{P}\{\hat{n} \geq n\} = (1 - \Pi_0)(1 - \Pi_1) \dots (1 - \Pi_{n-1}). \quad (\text{S72})$$

Setting  $\hat{\ell} = a\hat{n}$  and  $\ell = an$ , we get in the limit  $a \rightarrow 0$ :

$$\Psi(\ell) := \mathbb{P}\{\hat{\ell} > \ell\} = \exp(-K(\ell)), \quad (\text{S73})$$

where

$$K(\ell) := \frac{1}{D} \int_0^\ell d\ell' \kappa(\ell'), \quad (\text{S74})$$

with  $\kappa(\ell)$  being the reactivity at the local time  $\ell$ , i.e., an appropriate limit of  $\kappa_n$ . The reactivity  $\kappa(\ell)$  should be a non-negative function which is integrable in the vicinity of 0 to ensure  $\Psi(0) = 1$  (i.e.,  $\kappa(\ell)$  cannot diverge faster than  $\ell^{-\nu}$  as  $\ell \rightarrow 0$ , with  $\nu < 1$ ). When  $\kappa(\ell)$  is a constant  $\kappa_0$ , one gets  $K(\ell) = \kappa_0 \ell / D = q\ell$  and thus retrieves the exponential distribution of the stopping local time  $\hat{\ell}$ .

Taking the derivative of Eq. (S73), we get the probability density of the stopping local time  $\hat{\ell}$ :

$$\psi(\ell) = \frac{\kappa(\ell)}{D} \exp\left(-\frac{1}{D} \int_0^\ell d\ell' \kappa(\ell')\right). \quad (\text{S75})$$

Conversely, inverting Eq. (S75), we express the reactivity  $\kappa(\ell)$  as

$$\kappa(\ell) = D \frac{\psi(\ell)}{\int_\ell^\infty d\ell' \psi(\ell')}. \quad (\text{S76})$$

As a consequence, surface reaction mechanism can be selected by setting either the reactivity  $\kappa(\ell)$ , or the probability density  $\psi(\ell)$  of the stopping local time  $\hat{\ell}$ .

As discussed in the main text, the asymptotic behavior of  $\kappa(\ell)$  at large  $\ell$  distinguishes three scenarios:

(i) If  $\kappa(\ell)$  decreases slower than  $1/\ell$  (or increases), then  $K(\ell)$  diverges as a power law or faster,  $\psi(\ell)$  in Eq. (S75) exhibits a fast (typically stretched-exponential) decay in the limit  $\ell \rightarrow \infty$ , and thus all positive moments of  $\ell$  are finite, as in the conventional setting of a constant  $\kappa$ .

(ii) In the critical regime when  $\kappa(\ell)$  decays as  $\nu D/\ell$  (with some dimensionless constant  $\nu > 0$ ), Eq. (S75) implies that  $\psi(\ell) \propto \ell^{-1-\nu}$  so that only the moments of order smaller than  $\nu$  are finite; in particular, when  $\nu < 1$ , the mean  $\mathbb{E}\{\hat{\ell}\}$  is infinite, resulting in anomalous properties such as a power-law decay of the probability density of the reaction time in bounded domains (see Sec. SM.VI).

(iii) If  $\kappa(\ell)$  decreases faster than  $1/\ell$ ,  $K(\ell)$  approaches a finite limit  $K(\infty)$  and thus  $\Psi(\infty) = e^{-K(\infty)} > 0$ , i.e., the density  $\psi(\ell)$  is not normalized to 1; as a consequence, the stopping local time  $\hat{\ell}$  can be infinite with a finite probability,  $\mathbb{P}\{\hat{\ell} = \infty\} = \Psi(\infty)$ , i.e., the surface reaction may never occur in this case. This conclusion is rather expected: as the reactivity decreases fast, the particle that did not react at first encounters, has less and less chances to react at later ones.

#### SM.IV. GENERALIZED QUANTITIES

The alternative description developed in this work allows us to incorporate various surface reaction mechanisms via an appropriate stopping local time  $\hat{\ell}$ . In fact, the average of the full propagator  $P(\mathbf{x}, \ell, t|\mathbf{x}_0)$  with the probability  $\Psi(\ell) = \mathbb{P}\{\hat{\ell} > \ell\}$  of no surface reaction up to  $\ell$  yields a generalized propagator that accounts for the survival against the surface reaction determined by the stopping local time  $\hat{\ell}$  (i.e., for the condition  $\ell_t < \hat{\ell}$ ):

$$G_\psi(\mathbf{x}, t|\mathbf{x}_0) := \int_0^\infty d\ell \Psi(\ell) P(\mathbf{x}, \ell, t|\mathbf{x}_0). \quad (\text{S77})$$

Substituting the spectral expansion (S41) for the full propagator, we get in Laplace domain:

$$\begin{aligned} \tilde{G}_\psi(\mathbf{x}, p|\mathbf{x}_0) &= \tilde{G}_\infty(\mathbf{x}, p|\mathbf{x}_0) \\ &+ \frac{1}{D} \sum_n [V_n^{(p)}(\mathbf{x}_0)]^* V_n^{(p)}(\mathbf{x}) \int_0^\infty d\ell \Psi(\ell) e^{-\mu_n^{(p)} \ell}, \end{aligned} \quad (\text{S78})$$

where we used that  $\Psi(0) = 1$ . Integrating by parts, one can also write

$$\begin{aligned} \tilde{G}_\psi(\mathbf{x}, p|\mathbf{x}_0) &= \tilde{G}_\infty(\mathbf{x}, p|\mathbf{x}_0) \\ &+ \frac{1}{D} \sum_n [V_n^{(p)}(\mathbf{x}_0)]^* V_n^{(p)}(\mathbf{x}) \frac{1 - \Upsilon_\psi(\mu_n^{(p)})}{\mu_n^{(p)}}, \end{aligned} \quad (\text{S79})$$

where

$$\Upsilon_\psi(\mu) := \mathbb{E}\{e^{-\mu \hat{\ell}}\} = \int_0^\infty d\ell e^{-\mu \ell} \psi(\ell) \quad (\text{S80})$$

is the Laplace transform of the probability density  $\psi(\ell)$ . For the exponential law of  $\hat{\ell}$ , one has  $\Upsilon_\psi(\ell) = 1/(1 + \mu/q)$  and thus the conventional propagator admits the following spectral expansion:

$$\tilde{G}_q(\mathbf{x}, p|\mathbf{x}_0) = \tilde{G}_\infty(\mathbf{x}, p|\mathbf{x}_0) + \frac{1}{D} \sum_n \frac{[V_n^{(p)}(\mathbf{x}_0)]^* V_n^{(p)}(\mathbf{x})}{q + \mu_n^{(p)}}. \quad (\text{S81})$$

Setting  $q = 0$ , we obtain the identity

$$\frac{1}{D} \sum_n \frac{[V_n^{(p)}(\mathbf{x}_0)]^* V_n^{(p)}(\mathbf{x})}{\mu_n^{(p)}} = \tilde{G}_0(\mathbf{x}, p|\mathbf{x}_0) - \tilde{G}_\infty(\mathbf{x}, p|\mathbf{x}_0), \quad (\text{S82})$$

that helps us to rewrite Eq. (S79) alternatively as

$$\begin{aligned} \tilde{G}_\psi(\mathbf{x}, p|\mathbf{x}_0) &= \tilde{G}_0(\mathbf{x}, p|\mathbf{x}_0) \\ &- \frac{1}{D} \sum_n [V_n^{(p)}(\mathbf{x}_0)]^* V_n^{(p)}(\mathbf{x}) \frac{\Upsilon_\psi(\mu_n^{(p)})}{\mu_n^{(p)}}. \end{aligned} \quad (\text{S83})$$

As previously, the normal derivative of the propagator defines the probability flux density  $j_\psi(\mathbf{s}, t|\mathbf{x}_0)$ :

$$j_\psi(\mathbf{s}, t|\mathbf{x}_0) := -D(\partial_n G_\psi(\mathbf{x}, t|\mathbf{x}_0))|_{\mathbf{x}=\mathbf{s}}. \quad (\text{S84})$$

The latter can also be expressed in terms of the surface hopping propagator. For this purpose, one can multiply the boundary condition (S49) by  $\Psi(\ell)$  and integrate over  $\ell$  from 0 to  $\infty$  to get

$$\begin{aligned} -D(\partial_n G_\psi(\mathbf{x}, t|\mathbf{x}_0))|_{\mathbf{x}=\mathbf{s}} &= j_\infty(\mathbf{s}, t|\mathbf{x}_0) \\ &+ D \int_0^\infty d\ell \Psi(\ell) \partial_\ell P(\mathbf{s}, \ell, t|\mathbf{x}_0), \end{aligned}$$

where we used that  $\Psi(0) = 1$ . The integration by parts yields

$$-D(\partial_n G_\psi(\mathbf{x}, t|\mathbf{x}_0))|_{\mathbf{x}=\mathbf{s}} = \int_0^\infty d\ell \psi(\ell) DP(\mathbf{s}, \ell, t|\mathbf{x}_0), \quad (\text{S85})$$

where we used Eq. (S50) and the regularity condition (S51). We conclude thus

$$j_\psi(\mathbf{s}, t|\mathbf{x}_0) = \int_0^\infty d\ell \psi(\ell) DP(\mathbf{s}, \ell, t|\mathbf{x}_0). \quad (\text{S86})$$

It is instructive to re-write Eq. (S85) as

$$\int_0^\infty d\ell \left( \Psi(\ell) (\partial_n P(\mathbf{x}, \ell, t|\mathbf{x}_0))|_{\mathbf{x}=\mathbf{s}} + \psi(\ell) P(\mathbf{s}, \ell, t|\mathbf{x}_0) \right) = 0. \quad (\text{S87})$$

If  $\psi(\ell) = qe^{-q\ell}$  (and thus  $\Psi(\ell) = e^{-q\ell}$ ), this identity implies the Robin boundary condition (S11) for the conventional propagator. However, for other distributions of the stopping local time  $\hat{\ell}$ , the generalized propagator  $G_\psi(\mathbf{x}, t|\mathbf{x}_0)$  does not satisfy the Robin boundary condition (S11), i.e.,  $G_\psi(\mathbf{s}, t|\mathbf{x}_0)$  is not proportional to  $j_\psi(\mathbf{s}, t|\mathbf{x}_0)$ . In other words, setting the reactive flux density in Eq. (S11) to be proportional to  $G_q(\mathbf{s}, t|\mathbf{x}_0)$  was a *choice*, one among many others. This choice represented the constant surface reactivity  $\kappa$ . Expressing  $\psi(\ell)$  and  $\Psi(\ell)$  in terms of  $\kappa(\ell)$  and  $K(\ell)$  via Eq. (S75), one can also write Eq. (S87) as

$$\int_0^\infty d\ell e^{-K(\ell)} \left( [D\partial_n + \kappa(\ell)]P(\mathbf{x}, \ell, t|\mathbf{x}_0) \right) \Big|_{\mathbf{x}=\mathbf{s}} = 0, \quad (\text{S88})$$

which can be seen as an extension of the Robin boundary condition to the case of encounter-dependent reactivity  $\kappa(\ell)$ . We emphasize that the integral form of this relation cannot be relaxed, given that the full propagator  $P(\mathbf{x}, \ell, t|\mathbf{x}_0)$  is unrelated to surface reaction.

The Laplace transform of Eq. (S86) with respect to  $t$  yields

$$\tilde{j}_\psi(\mathbf{s}, p|\mathbf{x}_0) = \int_0^\infty d\ell \psi(\ell) D\tilde{P}(\mathbf{s}, \ell, p|\mathbf{x}_0). \quad (\text{S89})$$

This expression naturally extends Eq. (S26) to any distribution of the stopping local time  $\hat{\ell}$ . The spectral expansion (S40) implies

$$\tilde{j}_\psi(\mathbf{s}, p|\mathbf{x}_0) = \sum_n [V_n^{(p)}(\mathbf{s}_0)]^* v_n^{(p)}(\mathbf{s}) \Upsilon_\psi(\mu_n^{(p)}), \quad (\text{S90})$$

where  $\Upsilon_\psi(\mu)$  is given by Eq. (S80).

As in the conventional setting, the probability flux density  $j_\psi(\mathbf{s}, t|\mathbf{x}_0)$  is the joint probability density of the reaction location  $\mathbf{X}_\mathcal{T}$  and of the reaction time  $\mathcal{T}$ . As a consequence, the integral of  $j_\psi(\mathbf{s}, t|\mathbf{x}_0)$  over  $t$  gives the marginal probability density of the reaction position (the so-called spread harmonic measure in the conventional setting [67, 68]):

$$\omega_\psi(\mathbf{s}|\mathbf{x}_0) := \int_0^\infty dt j_\psi(\mathbf{s}, t|\mathbf{x}_0) = \tilde{j}_\psi(\mathbf{s}, 0|\mathbf{x}_0), \quad (\text{S91})$$

whereas the integral of  $j_\psi(\mathbf{s}, t|\mathbf{x}_0)$  over  $\mathbf{s}$  yields the marginal probability density of the reaction time,

$$H_\psi(t|\mathbf{x}_0) := \int_{\partial\Omega} d\mathbf{s} j_\psi(\mathbf{s}, t|\mathbf{x}_0). \quad (\text{S92})$$

Substituting Eq. (S90), we get

$$\begin{aligned} \omega_\psi(\mathbf{s}|\mathbf{x}_0) &= \int_0^\infty d\ell \psi(\ell) D\tilde{P}(\mathbf{s}, \ell, 0|\mathbf{x}_0) \\ &= \sum_n [V_n^{(0)}(\mathbf{x}_0)]^* \Upsilon_\psi(\mu_n^{(0)}) v_n^{(0)}(\mathbf{s}) \end{aligned} \quad (\text{S93})$$

and

$$\tilde{H}_\psi(p|\mathbf{x}_0) = \sum_n [V_n^{(p)}(\mathbf{x}_0)]^* \Upsilon_\psi(\mu_n^{(p)}) \int_{\partial\Omega} d\mathbf{s} v_n^{(p)}(\mathbf{s}). \quad (\text{S94})$$

The Laplace-transformed survival probability follows as

$$\tilde{S}_\psi(p|\mathbf{x}_0) = \frac{1 - \tilde{H}_\psi(p|\mathbf{x}_0)}{p}. \quad (\text{S95})$$

Substituting Eqs. (S68, S89) into Eq. (S92), we get another representation

$$H_\psi(t|\mathbf{x}_0) = \int_0^\infty d\ell \psi(\ell) U(\ell, t|\mathbf{x}_0), \quad (\text{S96})$$

where  $U(\ell, t|\mathbf{x}_0)$  is the probability density of the first-crossing time. One can see that  $U(\ell, t|\mathbf{x}_0)$  plays a crucial role in determining the properties of the reaction time for *any surface reaction mechanism*, the latter being encoded via the density  $\psi(\ell)$  of the stopping local time  $\hat{\ell}$ . As the full propagator  $P(\mathbf{x}, \ell, t|\mathbf{x}_0)$  is the fundamental intrinsic characteristics of reflected Brownian motion, from which the conventional propagator  $G_q(\mathbf{x}, t|\mathbf{x}_0)$  follows via the Laplace transform (S14), the probability density  $U(\ell, t|\mathbf{x}_0)$  is the fundamental intrinsic characteristics of the boundary local time, from which  $H_\psi(t|\mathbf{x}_0)$  follows via Eq. (S96). In particular, the conventional density  $H_q(t|\mathbf{x}_0)$  is obtained for the exponential stopping local time:

$$H_q(t|\mathbf{x}_0) = \int_0^\infty d\ell qe^{-q\ell} U(\ell, t|\mathbf{x}_0), \quad (\text{S97})$$

from which one can also express  $U(\ell, t|\mathbf{x}_0)$  as the inverse Laplace transform with respect to  $q$ :

$$U(\ell, t|\mathbf{x}_0) = \mathcal{L}_\ell^{-1}\{H_q(t|\mathbf{x}_0)/q\}. \quad (\text{S98})$$

When there are many independent particles distributed with an initial concentration  $c(\mathbf{x}_0)$ , their total diffusive flux, or the reaction rate  $J_\psi(t)$ , can be obtained by averaging the probability fluxes from all starting points  $\mathbf{x}_0$  in the bulk:

$$J_\psi(t) := \int_\Omega d\mathbf{x}_0 c(\mathbf{x}_0) H_\psi(t|\mathbf{x}_0). \quad (\text{S99})$$

For a uniform concentration,  $c(\mathbf{x}_0) = c_0$ , we use the identity from [27]

$$\int_{\Omega} d\mathbf{x}_0 V_n^{(p)}(\mathbf{x}_0) = \frac{D}{p} \mu_n^{(p)} \int_{\partial\Omega} d\mathbf{s} v_n^{(p)}(\mathbf{s}) \quad (\text{S100})$$

to write

$$\tilde{J}_{\psi}(p) = \frac{c_0 D}{p} \sum_n \left| \int_{\partial\Omega} d\mathbf{s} v_n^{(p)}(\mathbf{s}) \right|^2 \mu_n^{(p)} \Upsilon_{\psi}(\mu_n^{(p)}). \quad (\text{S101})$$

One can also represent the reaction rate as

$$J_{\psi}(t) = \int_0^{\infty} d\ell \psi(\ell) U_{\text{uni}}(\ell, t), \quad (\text{S102})$$

where  $U_{\text{uni}}(\ell, t)$  is given by the inverse Laplace transform of

$$\begin{aligned} \tilde{U}_{\text{uni}}(\ell, p) &:= c_0 \int_{\Omega} d\mathbf{x}_0 \tilde{U}(\ell, p|\mathbf{x}_0) \\ &= \frac{c_0 D}{p} \sum_n \mu_n^{(p)} e^{-\mu_n^{(p)} \ell} \left| \int_{\partial\Omega} d\mathbf{s} v_n^{(p)}(\mathbf{s}) \right|^2. \end{aligned} \quad (\text{S103})$$

The above expressions couple the diffusive dynamics determined by the eigenvalues and eigenfunctions of the Dirichlet-to-Neumann operator to the surface reaction mechanism determined by  $\Upsilon_{\psi}(\mu)$ .

We also mention that the symmetry of some domains can imply that the ground eigenfunction  $v_0^{(p)}(\mathbf{s})$  is constant, whereas other eigenfunctions should be orthogonal to it (see Sec. SM.V for the example of a spherical shell). In this special case, the spectral expansions (S94, S101) are reduced to a single term depending on  $\mu_0^{(p)}$ , whereas a general surface reaction mechanism encoded by the function  $\Upsilon_{\psi}(\mu)$  is formally equivalent to a partially reactive surface with a “frequency”-dependent reactivity  $\kappa_{\text{eff}}(p)$  defined by

$$\frac{1}{1 + \mu_0^{(p)} D / \kappa_{\text{eff}}(p)} = \Upsilon_{\psi}(\mu_0^{(p)}). \quad (\text{S104})$$

In time domain, such a reactivity corresponds to a convolution-type Robin boundary condition. While the above relation may provide an additional insight onto our generalized surface reaction mechanisms, this “equivalence” is very specific and valid only when a single eigenmode contributes, e.g., for the probability density  $H_{\psi}(t|\mathbf{x}_0)$  and the associated reaction rate  $J_{\psi}(t)$  in selected symmetric domains.

## SM.V. SPHERICAL SHELL

As an important practical example, we consider a spherical shell between two concentric spheres of radii

$R$  and  $L$ :  $\Omega = \{\mathbf{x} \in \mathbb{R}^3 : R < |\mathbf{x}| < L\}$ . While different combinations of boundary conditions are possible, we focus on the typical case when the reactive target of radius  $R$  is confined by an outer reflecting boundary of radius  $L$ . The rotational invariance of  $\Omega$  implies that the eigenfunctions of the Dirichlet-to-Neumann operator, written in spherical coordinates  $(r, \theta, \phi)$ , are the (normalized) spherical harmonics (see [27, 41] for details),

$$v_{nm}(\mathbf{s}) = \frac{1}{R} Y_{mn}(\theta, \phi) \quad (n = 0, 1, 2, \dots, |m| \leq n), \quad (\text{S105})$$

which are independent of  $p$ . In turn, the eigenvalues are

$$\mu_n^{(p)} = -g_n'(R), \quad (\text{S106})$$

where

$$g_n(r) = \frac{k_n'(\alpha L) i_n(\alpha r) - i_n'(\alpha L) k_n(\alpha r)}{k_n'(\alpha L) i_n(\alpha R) - i_n'(\alpha L) k_n(\alpha R)}, \quad (\text{S107})$$

$\alpha = \sqrt{p/D}$ , prime denotes the derivative with respect to the argument, and  $i_n(z)$  and  $k_n(z)$  are the modified spherical Bessel functions of the first and second kind, respectively. We emphasize that the Dirichlet-to-Neumann operator is associated here to the boundary local time exclusively on the inner sphere. The eigenvalue  $\mu_n^{(p)}$  is  $(2n+1)$  times degenerate. In the limit  $L \rightarrow \infty$ , one gets

$$\mu_n^{(p)} = -\sqrt{p/D} \frac{k_n'(R\sqrt{p/D})}{k_n(R\sqrt{p/D})} \quad (\text{S108})$$

for the exterior of a ball. In the limit  $p \rightarrow 0$ , one has

$$\mu_n^{(0)} = \frac{n+1}{R} \frac{1 - (R/L)^{2n+1}}{1 + \frac{n+1}{n} (R/L)^{2n+1}}, \quad (\text{S109})$$

which reduces to  $(n+1)/R$  as  $L \rightarrow \infty$ .

One also needs to compute  $V_n^{(p)}(\mathbf{x}_0)$  from Eq. (S42). Using the summation formulas from [69], the Laplace-transformed propagator  $\tilde{G}_{\infty}(\mathbf{x}, p|\mathbf{x}_0)$  and thus  $\tilde{j}_{\infty}(\mathbf{s}, p|\mathbf{x}_0)$  for a spherical shell with Dirichlet boundary condition on the inner sphere and Neumann boundary condition on the outer sphere read

$$\begin{aligned} \tilde{G}_{\infty}(\mathbf{x}, p|\mathbf{x}_0) &= \sum_{n=0}^{\infty} \frac{\alpha(2n+1)}{4\pi D} P_n\left(\frac{\mathbf{x} \cdot \mathbf{x}_0}{|\mathbf{x}||\mathbf{x}_0|}\right) g_n(r_0) \\ &\quad \times [k_n(\alpha R) i_n(\alpha r) - i_n(\alpha R) k_n(\alpha r)], \end{aligned} \quad (\text{S110})$$

$$\tilde{j}_{\infty}(\mathbf{s}, p|\mathbf{x}_0) = \sum_{n=0}^{\infty} \frac{2n+1}{4\pi R^2} P_n\left(\frac{\mathbf{s} \cdot \mathbf{x}_0}{|\mathbf{s}||\mathbf{x}_0|}\right) g_n(r_0), \quad (\text{S111})$$

where  $r = |\mathbf{x}|$ ,  $r_0 = |\mathbf{x}_0|$ ,  $R \leq r \leq r_0 \leq L$ ,  $P_n(z)$  are the Legendre polynomials, and we used the Wronskian  $i_n'(z)k_n(z) - k_n'(z)i_n(z) = 1/z^2$ . The projection of  $\tilde{j}_{\infty}(\mathbf{s}, p|\mathbf{x}_0)$  onto an eigenfunction  $v_{nm}(\mathbf{s})$  from Eq. (S105) reads then

$$V_{nm}^{(p)}(\mathbf{x}_0) = v_{nm}(\theta_0, \phi_0) g_n(r_0). \quad (\text{S112})$$

The orthogonality of spherical harmonics reduces Eq. (S69) to

$$U(\ell, t|\mathbf{x}_0) = \mathcal{L}_t^{-1}\{g_0(r_0) \exp(-\mu_0^{(p)} \ell)\}, \quad (\text{S113})$$

while the probability density of the reaction time reads

$$H_\psi(t|\mathbf{x}_0) = \mathcal{L}_t^{-1}\{g_0(r_0) \Upsilon_\psi(\mu_0^{(p)})\}, \quad (\text{S114})$$

where

$$\begin{aligned} \mu_0^{(p)} &= (\alpha + 1/R) \frac{1 - v(R) \frac{e^{-2\alpha R} + (\alpha R - 1)/(\alpha R + 1)}{1 - e^{-2\alpha R}}}{1 + v(R)}, \\ g_0(r_0) &= \frac{R}{r_0} e^{-\alpha(r_0 - R)} \frac{1 + v(r_0)}{1 + v(R)}, \\ v(r) &= e^{-2\alpha(L-r)} \frac{1 - e^{-2\alpha r}}{e^{-2\alpha L} + \frac{\alpha L - 1}{\alpha L + 1}}. \end{aligned}$$

Similarly, Eq. (S103) reads

$$U_{\text{uni}}(\ell, t) = 4\pi R^2 c_0 D \mathcal{L}_t^{-1}\left\{\frac{\mu_0^{(p)}}{p} \exp(-\mu_0^{(p)} \ell)\right\}. \quad (\text{S115})$$

## SM.VI. SURFACE REACTION MODELS

In this section, we discuss several models of surface reaction mechanisms, which are determined by choosing an appropriate distribution for the stopping local time  $\hat{\ell}$ . One can select either the probability density  $\psi(\ell)$  capturing the desired stopping criterion, or the desired dependence of the reactivity  $\kappa(\ell)$  on the local time  $\ell$ . According to Eqs. (S75, S76), both options are equivalent, i.e.,  $\psi(\ell)$  determines  $\kappa(\ell)$ , and vice-versa.

### A. Selected models

Table I lists selected distributions for the stopping local time  $\hat{\ell}$ , which can be used to produce a variety of surface reaction mechanisms (see also Fig. S3). Expectedly, only the exponential distribution of  $\hat{\ell}$  yields Poissonian-like reactions with a constant reactivity. Using the gamma distribution with the scale parameter  $\nu$ , one can either increase ( $\nu < 1$ ) or diminish ( $\nu > 1$ ) the probability of small values of  $\hat{\ell}$  and thus control the reactivity  $\kappa(\ell)$  at small local times. For  $\nu > 1$ , one can model reaction mechanisms, in which the surface is initially inactive and needs to be activated (“heated up”) by repeated encounters with the particle to start working with a constant reactivity. Alternatively, the gamma distribution with  $\nu < 1$  may describe situations when the surface is highly reactive at the beginning and then, after a number of encounters with the particle, reaches a lower constant reactivity.

In turn, a Pareto-type (or Lomax) distribution keeps the reactivity  $\kappa(\ell)$  constant at small  $\ell$  but then leads to

a power-law decay as  $1/\ell$  at large  $\ell$ . Such a distribution can model slow passivation (or aging) of the reactive surface due to repeated encounters with the particle. This example also illustrates that different densities  $\psi(\ell)$  (with different exponent  $\nu$ ) can result in a very similar behavior of the encounter-dependent reactivity  $\kappa(\ell)$  (which differ here only by a prefactor  $\nu$ ). Note that Mittag-Leffler distribution allows one to represent the decrease of reactivity even at small values of  $\ell$ .

More generally, Eq. (S75) helps one to incorporate a faster decay of the reactivity at large  $\ell$  such as a power law  $\ell^{-\nu}$  with  $\nu > 1$ , an exponential  $e^{-q\ell}$ , or any desired behavior. In this case, the probability density  $\psi(\ell)$  is not normalized to 1, and the surface reaction does not occur with the probability  $e^{-K(\infty)}$  (see Sec. SM.III). This is particularly clear for the truncated exponential distribution, for which the surface becomes totally inert after a number of encounters (when  $\ell > \ell_2$ ).

While previous examples provided monotonous behavior of the reactivity, the Lévy-Smirnov distribution results in a maximum of  $\kappa(\ell)$ . In this setting, the surface is almost inert for  $\ell \ll 1/q$ , becomes most reactive at  $\ell_c \approx 0.7667/q$ , and then slowly loses its reactivity. This model can describe surfaces that have an optimal range of reactivity.

Finally, the reactivity  $\kappa(\ell)$  can also be increasing with  $\ell$ . For instance, a linear asymptotic increase can be modeled by using one-sided Gaussian distribution of  $\hat{\ell}$ . Note that a faster increase of the reactivity implies a faster decrease of  $\psi(\ell)$  at large  $\ell$ .

### B. Reaction rate on a spherical target

Our probabilistic description couples the surface reaction mechanism to diffusive dynamics. In order to illustrate the effect of various mechanisms, we consider an archetypical setting in diffusion-mediated chemical kinetics – a spherical target of radius  $R$  in the three-dimensional space. For this target, Smoluchowski first derived the reaction rate for perfect reactions [70] and later Collins and Kimball extended it to partial reactivity [18].

The eigenvalues and eigenfunctions of the Dirichlet-to-Neumann operator for this domain are summarized in Sec. SM.V. The orthogonality of spherical harmonics removes all the terms in Eq. (S101), except the first one that gives

$$\tilde{J}_\psi(p) = J_S \frac{R}{p} \mu_0^{(p)} \Upsilon_\psi(\mu_0^{(p)}), \quad (\text{S116})$$

where  $\mu_0^{(p)} = \sqrt{p/D} + 1/R$  from Eq. (S108), and

$$J_S = 4\pi R c_0 D \quad (\text{S117})$$

is the steady-state Smoluchowski rate. For the conventional Poissonian-like surface reaction, one has  $\Upsilon(\mu) =$

n.	Distribution	$\psi(\ell)$	$\Upsilon_\psi(\mu)$	$\kappa(\ell)/\kappa_0$	$\ell \rightarrow 0$	$\ell \rightarrow \infty$	Comment
1	exponential	$qe^{-q\ell}$	$(1 + \mu/q)^{-1}$	1	1	1	
2	gamma	$qe^{-q\ell} \frac{(q\ell)^{\nu-1}}{\Gamma(\nu)}$	$(1 + \mu/q)^{-\nu}$	$\frac{(q\ell)^{\nu-1} e^{-q\ell}}{\Gamma(\nu, q\ell)}$	$\frac{(q\ell)^{\nu-1}}{\Gamma(\nu)}$	1	$\nu > 0$
3	Pareto II (Lomax)	$q\nu(1 + q\ell)^{-1-\nu}$	$\nu(\mu/q)^\nu e^{\mu/q}\Gamma(-\nu, \mu/q)$	$\nu/(1 + q\ell)$	$\nu$	$\nu/(q\ell)$	$\nu > 0$
4	Mittag-Leffler	$-E_{\nu,0}(-(q\ell)^\nu)/\ell$	$1/(1 + (\mu/q)^\nu)$	$(q\ell)^{\nu-1} \frac{E_{\nu,\nu}(-(q\ell)^\nu)}{E_{\nu,1}(-(q\ell)^\nu)}$	$\frac{(q\ell)^{\nu-1}}{\Gamma(\nu)}$	$\nu/(q\ell)$	$0 < \nu < 1$
5	power-law reactivity	$q\beta(1 + q\ell)^\nu \exp(\beta \frac{1-(1+q\ell)^{\nu+1}}{\nu+1})$	(see caption)	$\beta(1 + q\ell)^\nu$	$\beta$	$\beta(q\ell)^\nu$	$\nu \neq -1$
		$q\beta(q\ell)^\nu \exp(-\beta \frac{(q\ell)^{\nu+1}}{\nu+1})$	(see caption)	$\beta(q\ell)^\nu$	$\beta(q\ell)^\nu$	$\beta(q\ell)^\nu$	$\nu > -1$
6	exponential reactivity	$q\nu \exp(-q\ell - \nu(1 - e^{-q\ell}))$	$\frac{\nu M(\mu/q + 1, \mu/q + 2; \nu)}{e^\nu(\mu/q + 1)}$	$\nu \exp(-q\ell)$	$\nu$	$\nu e^{-q\ell}$	
7	truncated exponential	$qe^{-q(\ell-\ell_1)} \mathbb{I}_{(\ell_1, \ell_2)}(\ell)$	$e^{-\mu\ell_1} \frac{1 - e^{-(\mu+q)(\ell_2-\ell_1)}}{1 + \mu/q}$	$\mathbb{I}_{(\ell_1, \ell_2)}(\ell)$	0 or 1	0 or 1	$\ell_1 < \ell_2$
8	Lévy-Smirnov	$q \frac{\exp(-1/(q\ell))}{\sqrt{\pi} (q\ell)^{3/2}}$	$\exp(-2\sqrt{\mu/q})$	$\frac{\exp(-1/(q\ell))}{\sqrt{\pi} (q\ell)^{3/2} \text{erf}(\sqrt{1/(q\ell)})}$	$\sim e^{-1/(q\ell)}$	$1/(2q\ell)$	
9	one-sided Gaussian	$2q e^{-(q\ell)^2} / \sqrt{\pi}$	$\text{erfcx}(\mu/(2q))$	$\frac{2}{\sqrt{\pi} \text{erfcx}(q\ell)}$	$2/\sqrt{\pi}$	$2q\ell$	

TABLE I: Selected surface reaction models. The 2nd, 3rd and 4th columns present the probability density  $\psi(\ell)$ , its Laplace transform  $\Upsilon_\psi(\mu)$ , and the corresponding encounter-dependent reactivity  $\kappa(\ell)/\kappa_0$ , rescaled by some reference reactivity  $\kappa_0$  such that  $q = \kappa_0/D$ . The 5th and 6th columns show the leading term of the asymptotic behavior of  $\kappa(\ell)/\kappa_0$  at small and large  $\ell$ , respectively. Here  $\Gamma(\nu, z)$  is the upper incomplete gamma function;  $\text{erfcx}(z) = e^{z^2} \text{erfc}(z)$  is the scaled complementary error function;  $E_{\alpha,\beta}(z)$  is the Mittag-Leffler function;  $M(a, b; z) = {}_1F_1(a, b; z)$  is the Kummer's confluent hypergeometric function;  $\mathbb{I}_{(a,b)}(x)$  is the indicator function ( $\mathbb{I}_{(a,b)}(x) = 1$  if  $x \in (a, b)$  and 0 otherwise). For the model 5 (top line),  $\Upsilon_\psi(\mu) = \alpha\beta e^{\alpha\beta + \mu/q} \int_1^\infty dy e^{-\alpha\beta y - (\mu/q)y^\alpha}$  for  $\alpha > 0$  and  $\Upsilon_\psi(\mu) = |\alpha|\beta e^{\alpha\beta + \mu/q} \int_0^1 dy e^{-\alpha\beta y - (\mu/q)y^\alpha}$  for  $\alpha < 0$ , with  $\alpha = 1/(\nu + 1)$ . For the model 5 (bottom line),  $\Upsilon_\psi(\mu) = \alpha\beta \int_0^\infty dy e^{-\alpha\beta y - (\mu/q)y^\alpha}$ . For the Pareto-II model with  $\nu = 1/2$ , one can write  $\Upsilon_\psi(\mu) = 1 - \sqrt{\pi\mu/q} \text{erfcx}(\sqrt{\mu/q})$ .

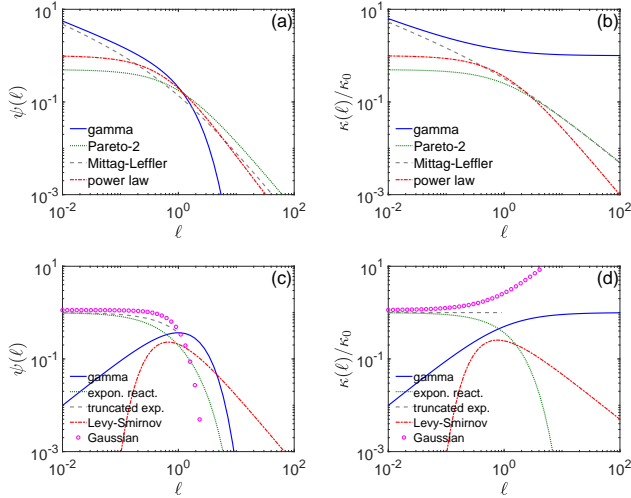


FIG. S3: Selected surface reaction models: **(a,c)** Probability density  $\psi(\ell)$  of the stopping local time  $\hat{\ell}$ ; **(b,d)** Encounter-dependent reactivity  $\kappa(\ell)/\kappa_0$ . Panels **(a,b)** present the gamma model ( $\nu = 0.5$ ), the Pareto-II model ( $\nu = 0.5$ ), the Mittag-Leffler model ( $\nu = 0.5$ ) and the power-law reactivity model ( $\nu = -1.5$ ). Panels **(c,d)** present the gamma model ( $\nu = 2$ ), the exponentially decaying reactivity model ( $\nu = 1$ ), the truncated exponential model ( $\ell_1 = 0, \ell_2 = 1$ ), the Lévy-Smirnov model, and the one-sided Gaussian model. In all cases,  $q = 1$ .

$1/(1 + \mu/q)$ , and the Laplace transform inversion of Eq. (S116) yields the Collins-Kimball's rate [18]:

$$\frac{J_q(t)}{J_S} = \frac{1}{1 + 1/(qR)} \left\{ 1 + qR \text{erfcx} \left( \sqrt{Dt} (q + 1/R) \right) \right\}, \quad (\text{S118})$$

where  $\text{erfcx}(z) = e^{z^2} \text{erfc}(z)$  is the scaled complementary error function. The function  $J_q(t)$  varies from the reaction-limited rate  $4\pi R^2 c_0 \kappa$  at  $t = 0$  to the diffusion-limited rate  $4\pi R c_0 D / (1 + 1/(qR))$  as  $t \rightarrow \infty$ . The limit  $q \rightarrow \infty$  gives the Smoluchowski's rate [70]:

$$\frac{J_\infty(t)}{J_S} = 1 + \frac{R}{\sqrt{\pi Dt}}. \quad (\text{S119})$$

For a general surface reaction mechanism, we perform the inverse Laplace transform of Eq. (S116) numerically by the Talbot algorithm.

The long-time behavior of the reaction rate, which is determined by the limit  $p \rightarrow 0$ , is universal. In fact, as  $\mu_0^{(p)}$  approaches a strictly positive constant  $\mu_0^{(0)} = 1/R$  in this limit, the reaction rate  $J_\psi(t)$  approaches its steady-state limit:

$$\frac{J_\psi(\infty)}{J_S} = \Upsilon_\psi(1/R) \leq 1. \quad (\text{S120})$$

In other words, all surface reaction mechanisms lead to a constant steady-state limit at long times, while the function  $\Upsilon_\psi(\mu)$  determines its level. We emphasize that this

is a general property for the exterior of any compact domain in  $\mathbb{R}^3$ , for which  $\mu_0^{(0)} > 0$  (even though in general, other terms in Eq. (S101) would contribute). In contrast, the way how  $J_\psi(t)$  reaches this limit, as well as the short-time behavior, are not universal.

We illustrate the effect of encounter-dependent reactivity onto the reaction rate by considering the gamma model (see Table I) which naturally generalizes the conventional exponential distribution. Figure S4 shows the reaction rate  $J_\psi(t)$  for a weakly reactive target with  $qR = 1$ . As discussed above, the shape parameter  $\nu$  determines the behavior of the reactivity  $\kappa(\ell)$  at small  $\ell$  and thus strongly affects the reaction rate at short times. Indeed, the short-time behavior of  $J_\psi(t)$  can be deduced from the asymptotic analysis of  $\tilde{J}_\psi(p)$  as  $p \rightarrow \infty$ :

$$\frac{J_\psi(t)}{J_S} = \frac{Rq^\nu}{\Gamma(\frac{\nu+1}{2})} (Dt)^{(\nu-1)/2} + O(t^{\nu/2}). \quad (\text{S121})$$

When  $\nu > 1$ , the reactivity  $\kappa(\ell)$  (see Table I) vanishes at small  $\ell$  so that the diffusing particle has low chances to react on the target at first encounters, and the reaction rate is accordingly small at short times. Only after a number of returns to the target, the reaction becomes probable that can model situations when the reactive surface needs to be progressively activated (“heated up”) by repeated encounters with the diffusing particle. The value  $\nu = 1$  corresponds to the conventional constant reactivity so that one retrieves the Collins-Kimball result (S118). In contrast, for  $0 < \nu < 1$ , the high reactivity at small  $\ell$  facilitates surface reactions at short times, enhancing the reaction rate. This setting can model surfaces which are highly reactive at the beginning and then reach a lower steady-state reactivity. Note also that in the limit  $\nu \rightarrow 0$ , the gamma distribution degenerates into a Dirac distribution  $\delta(\ell)$  so that this limit corresponds to a perfectly absorbing boundary, on which the reaction occurs at the first encounter. The reaction rate  $J_\psi(t)$  approaches thus  $J_\infty(t)$  from Eq. (S119).

### C. Distribution of the reaction time

The distribution of the reaction time  $\mathcal{T}$  on a target provides finer information about diffusion-influenced reactions. To go beyond the basic example of a spherical target in the whole space  $\mathbb{R}^3$ , we consider now a spherical target of radius  $R$  surrounded by an outer reflecting concentric sphere of radius  $L$  that confines diffusing particles within a bounded region around the target. In other words, we consider a spherical shell between two concentric spheres of radii  $R$  and  $L$  (see Sec. SM.V).

The distribution of the reaction time on a partially reactive target surrounded by an outer reflecting sphere has been thoroughly investigated for conventional Poissonian surface reaction (see [45] and references therein). Figure S5 presents the probability density  $H_\psi(t|\mathbf{x}_0)$  for several models of the surface reaction mechanism. Here

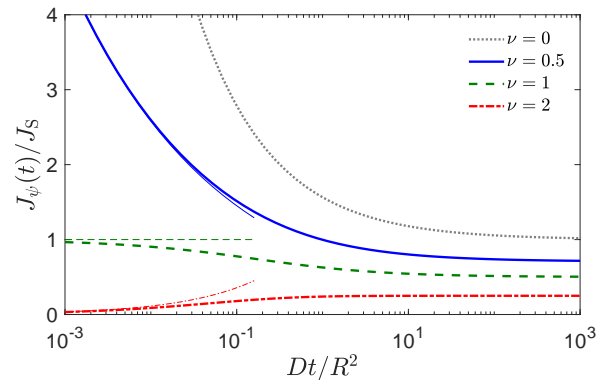


FIG. S4: The reaction rate  $J_\psi(t)$ , rescaled by the Smoluchowski steady-state rate  $J_S = 4\pi R c_0 D$ , on a spherical target of radius  $R$ , for the gamma distribution of the stopping local time  $\ell$ :  $\psi(\ell) = q(q\ell)^{\nu-1} e^{-q\ell} / \Gamma(\nu)$ , with  $qR = 1$  and three values of  $\nu$ :  $\nu = 0.5$  (solid line),  $\nu = 1$  (dashed line, Collins-Kimball rate  $J_q(t)$  from Eq. (S118)),  $\nu = 2$  (dash-dotted line). The associated thin lines present the short-time power law (S121) for these three cases. Dotted line shows the Smoluchowski rate  $J_\infty(t)$  from Eq. (S119) for a perfectly reactive target (limit  $\nu = 0$ ).

we fix  $|\mathbf{x}_0| = 2R$ ,  $L = 10R$  and  $qR = 1$ . Apart from the conventional exponential model, we consider the Lévy-Smirnov (LS) model, the Mittag-Leffler (ML) model, and the truncated exponential (TE) model with  $\ell_1 = 0$  and  $\ell_2 = 0.5R$ . In all cases,  $H_\psi(t|\mathbf{x}_0)$  is computed numerically via the inverse Laplace transform of Eq. (S114) evaluated by using the Talbot algorithm.

At short times, the probability density  $H_\psi(t|\mathbf{x}_0)$  for the ML and TE models is close to that of the exponential model. In fact, this behavior describes rare particles that move directly towards the target and rapidly react. Even though the reactivity  $\kappa(\ell)$  is increasing for the ML model, the overall reaction is still determined by diffusion. This situation is drastically different for the LS model, for which the reactivity  $\kappa(\ell)$  is extremely small at first encounters, thus shifting the probability density toward longer times. In turn, the LS and ML models, for which  $\psi(\ell)$  has the same power law decay as  $\ell \rightarrow \infty$  ( $\psi(\ell) \propto \ell^{-3/2}$ ), exhibit similar long-time behavior:

$$H_\psi(t|\mathbf{x}_0) \propto t^{-3/2} \quad (t \rightarrow \infty). \quad (\text{S122})$$

The power-law decay of  $H_\psi(t|\mathbf{x}_0)$  for a bounded domain is a new feature of the considered surface reaction mechanisms. The decreasing reactivity  $\kappa(\ell)$  facilitates the survival of particles even in bounded domains. A similar effect was earlier reported for continuous-time random walks in bounded domains [71], but it was related to long stalling periods that a particle experiences during its motion to the target. In our setting, the particle diffuses normally, and the enhancement of the survival probability is caused by the surface reaction mechanism. The long-time asymptotic formula (S122) is in

excellent agreement with  $H_\psi(t|\mathbf{x}_0)$ . Finally, in the case of the truncated exponential model, the probability density  $H_\psi(t|\mathbf{x}_0)$  decays exponentially again but it is not normalized to 1 anymore. In fact, as the boundary becomes inert for  $\ell > \ell_2$ , the particle that failed to react up to the boundary local time  $\ell_2$ , survives forever. In this example,  $\mathbb{P}\{\mathcal{T} = \infty\} = \exp(-q\ell_2) \approx 0.61$ .

We emphasize the generic character of the power-law decay of  $H_\psi(t|\mathbf{x}_0)$  in bounded domains in the critical regime when  $\kappa(\ell) \simeq \nu D/\ell$  at large  $\ell$  (with some dimensionless constant  $0 < \nu < 1$ ). In fact, the long-time asymptotic behavior of  $H_\psi(t|\mathbf{x}_0)$  is determined by the small- $p$  behavior of  $\tilde{H}_\psi(p|\mathbf{x}_0)$  and thus of  $\tilde{U}(\ell, p|\mathbf{x}_0)$ , due to Eq. (S96). For a bounded domain  $\Omega$ , the latter behavior is determined by the ground eigenmode, for which  $\mu_0^{(p)} \simeq \gamma p + O(p^2)$  as  $p \rightarrow 0$ , with  $\gamma = |\Omega|/(D|\partial\Omega|)$  [41]. As a consequence, we have

$$\tilde{U}(\ell, p|\mathbf{x}_0) \simeq \exp(-\gamma p \ell) \quad (p \rightarrow 0), \quad (\text{S123})$$

where we used that  $v_0^{(p)}(\mathbf{s}) \rightarrow |\partial\Omega|^{-1/2}$  as  $p \rightarrow 0$ , the orthogonality of other eigenfunctions  $v_n^{(p)}(\mathbf{s})$  to  $v_0^{(p)}(\mathbf{s})$ , and that  $V_0^{(p)}(\mathbf{x}_0) \rightarrow |\partial\Omega|^{-1/2}$ . Integrating the expression (S123) with  $\psi(\ell) \propto \ell^{-1-\nu}$  (see Sec. SM.III), one gets  $\tilde{H}_\psi(p|\mathbf{x}_0) \propto p^\nu$  as  $p \rightarrow 0$ , from which

$$H_\psi(t|\mathbf{x}_0) \propto t^{-1-\nu} \quad (t \rightarrow \infty). \quad (\text{S124})$$

The same asymptotic behavior holds for the reaction rate:  $J_\psi(t) \propto t^{-1-\nu}$ . Such a long-time asymptotic decay of the reaction time probability density is unusual for bounded domains, for which the conventional constant reactivity implies the exponential decay.

Figure S6 illustrates more explicitly the effect of truncated reactivity onto the reaction time distribution. In the top panel, we fix  $\ell_1 = 0$  and consider several values of  $\ell_2$ , i.e., the target is reactive at the beginning but becomes inert after a prescribed number of encounters with the particle. Expectedly, the overall shape of the probability density  $H_\psi(t|\mathbf{x}_0)$  does not change much but it is progressively reduced as  $\ell_2$  is getting smaller. This reduction results from the reduced normalization of  $\psi(\ell)$ , which is equal to  $1 - \Psi(\infty) = 1 - \exp(-q\ell_2)$ . For instance, for  $q\ell_2 = 0.1$ , the particle reacts only in 9.5% of cases, explaining a tenfold decrease of  $H_\psi(t|\mathbf{x}_0)$  in this case (dash-dotted line). In turn, the bottom panel of Fig. S6 presents the opposite situation when the target is passive at the beginning and becomes reactive after a prescribed number of encounters (i.e., we set  $\ell_1 > 0$  and  $\ell_2 = \infty$ ). The behavior of the probability density  $H_\psi(t|\mathbf{x}_0)$  is different. When  $\ell_1$  increases, more and more encounters with the target at the beginning do not produce surface reaction, shifting  $H_\psi(t|\mathbf{x}_0)$  towards longer times. Moreover, the shape of this density progressively transforms from monomodal to bimodal that is clearly seen at  $q\ell_1 = 5$ . In fact, the first maximum of  $H_\psi(t|\mathbf{x}_0)$  is located around the time of the order of  $(|\mathbf{x}_0| - R)^2/(6D) \simeq 0.17R^2/D$ , which is controlled by

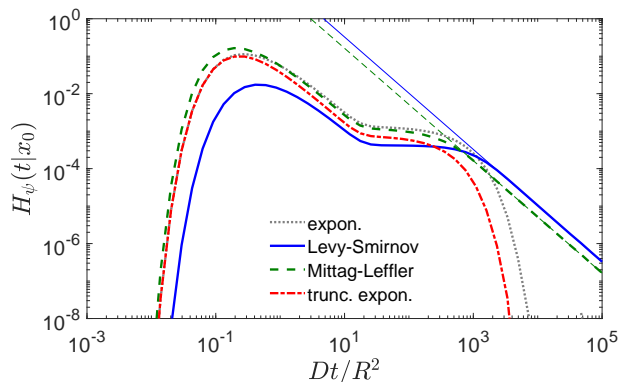


FIG. S5: The probability density  $H(t|\mathbf{x}_0)$  (rescaled by  $R^2/D$ ) of the reaction time on a spherical target of radius  $R$ , surrounded by an outer reflecting concentric sphere of radius  $L = 10R$ , for several surface reaction models and the starting point  $|\mathbf{x}_0| = 2R$ . Four models with  $qR = 1$  are compared: the conventional exponential model (dotted line), the Lévy-Smirnov model (solid line), the Mittag-Leffler model with  $\nu = 1/2$  (dashed line), and the truncated exponential model with  $\ell_1 = 0$  and  $\ell_2 = 0.5R$  (dash-dotted line). Thin lines show the long-time asymptotic behavior (S122) for the LS and ML models.

the distance to the target,  $|\mathbf{x}_0| - R$ . This maximum corresponds to direct trajectories from  $\mathbf{x}_0$  to the target (see discussion in [45] for the conventional case). As these rapid trajectories fail to produce surface reaction at first encounters with the inert target, the repeated returns to the target force the particle to explore the confining domain. As a result, the second maximum emerges around the mean reaction time on partially reactive target, which is of the order of  $L^3(|\mathbf{x}_0| - R + 1/q)/(3DR^2) \simeq 10^3 R^2/D$ . Such a bimodal shape of the probability density of the reaction time is again a new feature induced by the considered surface reaction mechanism.

## SM.VII. COMPARISON WITH BULK-MEDIATED SURFACE DIFFUSION

In a series of works, Chechkin *et al.* [46, 72, 73] and later Berezhkovskii *et al.* [47, 74] investigated bulk-mediated surface diffusion, which turns out to be complementary to our approach. In their model, a particle diffuses in the bulk with diffusion coefficient  $D_b$  until an encounter with the surface. After hitting the surface, a particle can either resume bulk diffusion or be adsorbed and start surface diffusion with diffusion coefficient  $D_s$ . After a random exponentially distributed time, the particle desorbs from the surface and starts bulk diffusion again, until the next adsorption. This model enters the class of “facilitated diffusions” [75] and was often employed in chemical physics to describe reversible reactions [76, 77], whereas first-passage times of the associated in-

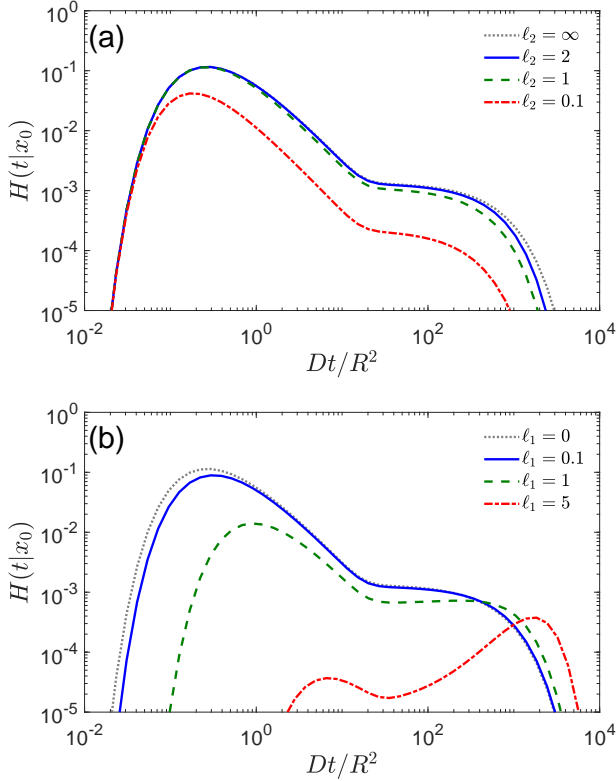


FIG. S6: The probability density  $H_\psi(t|\mathbf{x}_0)$  (rescaled by  $R^2/D$ ) of the reaction time on the spherical target of radius  $R$  surrounded by an outer reflecting concentric sphere of radius  $L = 10R$ , with  $|\mathbf{x}_0| = 2R$ . We consider the truncated reactivity model with: (a)  $\ell_1 = 0$  and several  $\ell_2$ , and (b) several  $\ell_1$  and  $\ell_2 = \infty$ . In all cases,  $qR = 1$ .

termittent process were thoroughly investigated [78–83].

For cylindrical and planar domains, Chechkin *et al.* solved coupled bulk and surface diffusion equations with exchange at the surface and obtained an effective surface propagator  $n_s(\mathbf{s}, t)$  characterizing the displacements of particles in the adsorbed state on the surface. For instance, in the case of a planar surface, this propagator in the Laplace-Fourier domain reads [73] (see Eq. (A6)):

$$n_s(\mathbf{k}, p) = \frac{1}{p + D_s|\mathbf{k}|^2 + \tau_{\text{des}}^{-1}[1 - W_{\text{bulk}}(\mathbf{k}, p)]}, \quad (\text{S125})$$

where  $\mathbf{k}$  is the Fourier vector associated to  $\mathbf{s}$ ,  $\tau_{\text{des}}$  is the mean desorption time, and  $W_{\text{bulk}}(\mathbf{k}, p)$  describes a bulk-mediated excursion over a partially reactive surface. This function can be obtained by averaging our surface hopping propagator  $\Sigma_p(\mathbf{s}, \hat{\ell}|\mathbf{s}_0)$  over the stopping local time  $\hat{\ell}$  with exponential density  $qe^{-q\hat{\ell}}$ . In our notations, it reads

$$\begin{aligned} W_{\text{bulk}}(\mathbf{k}, p) &= \mathcal{F}_{\mathbf{k}}\{\mathbb{E}\{\Sigma_p(\mathbf{s}, \hat{\ell}|\mathbf{s}_0)\}\} \\ &= \frac{1}{1 + \frac{1}{q}\sqrt{|\mathbf{k}|^2 + p/D_b}}, \end{aligned} \quad (\text{S126})$$

in agreement with Eq. (A5) from [73], where the coefficient  $\mu D_b \tau_{\text{des}} = a$  is identified with  $1/q$ , and  $\mathcal{F}_{\mathbf{k}}$  denotes the Fourier transform with respect to  $\mathbf{s} - \mathbf{s}_0$ . In the double limit  $\tau_{\text{des}} \rightarrow 0$  and  $a \rightarrow 0$  (such that  $\mu$  is kept constant), Eq. (S125) yields the effective surface propagator on the plane:

$$n_s(\mathbf{k}, p) = \frac{1}{p + D_s|\mathbf{k}|^2 + \mu D_b \sqrt{|\mathbf{k}|^2 + p/D_b}}. \quad (\text{S127})$$

The properties of this propagator have been thoroughly investigated in [73]. We stress a significant difference between this propagator and the surface hopping propagator  $\Sigma_p(\mathbf{s}, \ell|\mathbf{s}_0)$  that we introduced. For instance, we obtain in the Laplace-Fourier domain:

$$\mathcal{F}_{\mathbf{k}}\{\Sigma_p(\mathbf{s}, \ell|\mathbf{s}_0)\} = \exp(-\ell\sqrt{|\mathbf{k}|^2 + p/D_b}), \quad (\text{S128})$$

which clearly differs from Eq. (S127), even in the case of no surface diffusion ( $D_s = 0$ ).

Berezhkovskii *et al.* analyzed coupled bulk-surface diffusion on a flat surface by focusing on the cumulative residence times spent by the particle in the two states [47, 74]. They also derived the propagator in the Laplace-Fourier space, which reads in our notations as

$$Q(\mathbf{k}, p) = \frac{1 + \frac{1}{q}\sqrt{|\mathbf{k}|^2 + p/D_b}}{p + D_s|\mathbf{k}|^2 + (p + D_s|\mathbf{k}|^2 + \tau_{\text{des}}^{-1})\frac{1}{q}\sqrt{|\mathbf{k}|^2 + \frac{p}{D_b}}}, \quad (\text{S129})$$

where  $q = \kappa/D_b$ . This propagator could be directly deduced via a renewal approach by summing the geometric series with bulk and surface propagators:

$$Q(\mathbf{k}, p) = \frac{\tau_{\text{des}} Q_s(\mathbf{k}, p)}{1 - Q_s(\mathbf{k}, p)W_{\text{bulk}}(\mathbf{k}, p)}, \quad (\text{S130})$$

with  $Q_s(\mathbf{k}, p) = 1/(1 + \tau_{\text{des}}(p + D_s|\mathbf{k}|^2))$  describing surface diffusion. We note that this approach differs from that by Chechkin *et al.* as there is no double limit  $q \rightarrow \infty$  and  $\tau_{\text{des}} \rightarrow 0$ .

In spite of this minor difference, both above approaches rely on coupled bulk-surface diffusion, whereas our description focuses exclusively on bulk excursions between encounters with the surface, without absorption/desorption kinetics. This description naturally involves the boundary local time  $\ell$  instead of physical time  $t$  in the effective surface propagator. As our description characterizes reflections on the boundary before each successful binding, it may provide deeper insights onto the intermittent dynamics and complement the former approaches.

## SM.VIII. DESCRIPTION OF FIGURE 1

In this section, we provide some technical descriptions of Fig. 1 in the main text.

The surface was generated by a freely available custom matlab routine that produces a rough landscape with prescribed Hurst exponent  $H$ , root-mean-square roughness  $\sigma_S$ , and number of pixels  $M$  [84]. We set  $H = 0.95$  and  $\sigma_S = 0.05$  to get mildly rough surface of fractal dimension  $3 - H = 2.05$  and of size  $1024 \times 1024$  pixels. It was rescaled to get variations along  $x$  and  $y$  coordinates between 0 and 1. Note that other types of surfaces and other codes could be used for our illustrative purpose.

The random trajectory was simulated by our custom matlab routine that generates independent three-dimensional Gaussian displacements with  $D = 1$  and timestep  $\tau = 10^{-6}$  to have the standard deviation  $\sigma = \sqrt{2D\tau} \approx 1.41 \cdot 10^{-3}$  along each coordinate. The initial point (red ball) was fixed at  $(0.5, 0.5, Z(0.5, 0.5) + h)$ , where  $Z(x, y)$  is the height of the surface at  $(x, y)$ , and  $h$  is a prescribed starting distance fixed at  $h = 0.3$ . At each ( $k$ -th) step, it is checked whether the newly generated position  $(x_k, y_k, z_k)$  lies above the surface, i.e.,  $z_k \geq Z(x_k, y_k)$ . In the opposite case, the  $z$  coordinate is updated to be  $z_k = Z(x_k, y_k) + a$ , with  $a = 10^{-2}$ . This change implements a reflection from the surface after an encounter (such encounter points are shown by blue and

yellow balls). Reflecting boundary conditions were also imposed at planes  $x = 0$ ,  $x = 1$ ,  $y = 0$ , and  $y = 1$  but we selected a trajectory that did not experience such constraints. A random trajectory with  $10^5$  points was generated.

The surface points  $(x, y, Z(x, y))$  were colored by using the function

$$\Sigma_0(x, y, \ell | x_1, y_1) = \frac{\ell}{2\pi[\ell^2 + (x - x_1)^2 + (y - y_1)^2]^{3/2}}, \quad (\text{S131})$$

where  $(x_1, y_1, Z(x_1, y_1))$  is the first arrival position on the surface, and  $\ell = 0.3$  is a prescribed parameter. This function is maximal (dark red) near the first arrival point and then gradually decreases as  $(x, y)$  is getting farther from  $(x_1, y_1)$  (dark blue). If the surface was a plane, the function  $\Sigma_0$  would be the surface hopping propagator from  $(x_1, y_1)$  to  $(x, y)$  within the local time  $\ell$ . This is no more the case for a rough surface shown in Fig. 1 but  $\Sigma_0$  may still be considered as a lowest-order crude approximation of the surface hopping propagator. It aims just to illustrate the basic idea behind this concept.